Journal of Applied Polymer Science

REVIEW

Graphene and Graphene Oxide and Their Uses in Barrier Polymers

Byung Min Yoo, Hye Jin Shin, Hee Wook Yoon, Ho Bum Park
Department of Energy Engineering, Hanyang University, Seoul 133-791, Republic of Korea
Correspondence to: H. B. Park (E-mail: badtzhb@hanyang.ac.kr)

ABSTRACT: Currently, there is great interest in graphene-based devices and applications because graphene has unique electronic and material properties, which can lead to enhanced material performance. Graphene may be used in a wide variety of potential applications from next-generation transistors to lightweight and high-strength polymeric composite materials. Graphene, which has atomic thickness and two-dimensional sizes in the tens of micrometer range or larger, has also been considered a promising nanomaterial in gas- or liquid-barrier applications because perfect graphene sheets do not allow diffusion of small gases or liquids through its plane. Recent molecular simulations and experiments have demonstrated that graphene and its derivatives can be used for barrier applications. In general, graphene and its derivatives can be applied via two major routes for barrier polymer applications. One is the transfer or coating of few-layered, ultrathin graphene and its derivatives, such as graphene oxide (GO) and reduced graphene oxide (rGO), on polymeric substrates. The other is the incorporation of fully exfoliated GO or rGO nanosheets into the polymeric matrix. In this article, we review the state-of-the-art research on the use of graphene, GO, and rGO for barrier applications, including few-layered graphene or its derivatives in coated polymeric films and polymer nanocomposites consisting of chemically exfoliated GO and rGO nanosheets, and their gas-barrier properties. As compared to other nanomaterials being used for barrier applications, the advantages and current limitations are discussed to highlight challenging issues for future research and the potential applications of graphene/polymer, GO/polymer, and rGO/polymer composites. © 2013 Wiley Periodicals, Inc. J. Appl. Polym. Sci. 000: 000–000, 2013

KEYWORDS: composites; graphene and fullerenes; nanotubes; nonpolymeric materials and composites; packaging

Received 28 April 2013; accepted 4 June 2013; Published online
DOI: 10.1002/app.39628

INTRODUCTION

Barrier polymers have become more and more important in many packaging and protective applications, such as in the food industry,[1,2] pharmaceuticals, and electronic devices, such as flexible displays.[3,4] Barrier polymers for packaging applications should have ultralow gas and water-vapor permeabilities or selective gas permeability in various environments, as shown in Figure 1(a). In particular, electronic devices, such as organic light-emitting diodes (OLEDs), are very vulnerable to moisture and oxygen because of the encapsulated light-emitting materials.[3] They consist of conjugated molecules and are degraded when they come into contact with water or oxygen; therefore, OLED requires passivation to protect itself. Currently, most displays have metal or glass protection encapsulating the devices.[4] If OLEDs are kept with a passivation layer with a polymeric gas-barrier film; instead, the thickness of the display can be drastically thinned, even close to the substrates. Moreover, a high mechanical strength, optical transparency, and thermal and chemical stability should also be necessary for ideal packaging applications. Currently, there are a number of methods for improving barrier properties in polymeric materials, but they still suffer from some drawbacks, including a high cost, humidity sensitivity, opacity, and low mechanical strength.[5] The most common method is to coat thin-film polymers[5–7] with low-gas-permeable barrier polymers, such as polyethylene (PE),[8] polypropylene (PP),[9] poly(ethylene terephthalate) (PET),[10] and poly(vinyl alcohol) (PVA).[11] However, even though such polymers are light, inexpensive, and easily processable, their applications as barriers are often limited because of a relatively high gas permeability as compared to high-criteria demands for modern packaging applications. Figure 1(a) shows the water vapor transmission rate (WVTR) and oxygen transmission rate (OTR) of common organic polymers used for barrier applications.[5] The gas-barrier performance of some polymers would satisfy food packaging criteria; however, they are still insufficient for current display devices, such as OLEDs and liquid crystal displays (LCD), and vacuum-insulating applications. Another promising technique is inorganic and organic multiple layer coating methods[12] by atomic layer deposition [ALD; Figure 1(b)] or molecular layer deposition [MLD; Figure 1(c)]. Such multilayered inorganic materials exhibit extremely low WVTRs ($<10^{-6}$ g/m^2 day), which are quite suitable for use in OLED protective layers.[13,14] However, ALD and MLD are very expensive, and their broad application is still limited because of a

lack of scale-up. Moreover, deposited inorganic layers often include unfavorable defects[15,16] that allow the transmission of permeants such as water and oxygen through such defective sites. Accordingly, many studies to overcome the disadvantages have been conducted to develop improved packaging materials with a highly gas-impermeable nature.

Recently, graphene has gained significant attention and has become one of the most widely investigated materials because of its superior material properties. In addition, graphene, a monolayer of graphite, is considered an ultrathin, perfect two-dimensional (2D) barrier against gas diffusion.[17,18] Ideally, defect-free, single-crystalline, monolayer graphene has not only excellent mechanical properties[19] and high transparency[20] but is also gas-impermeable. However, the synthesis of large-area, defect-free, single-crystalline, monolayer graphene is still extremely challenging.[21–23] One strategy for the use of the gas-barrier properties of graphene in mass production is to use graphene oxide (GO) and its reduced form [reduced graphene oxide (rGO)]. Namely, GO thin layers can be coated on desirable polymeric substrates for barrier applications. GO consists of oxygen-containing functional groups on the basal plane,[24] and it can be well-dispersed in aqueous polar solvents such as water; this results in scalable mass production.[25,26] However, GO contains some defects on its basal plane; therefore, multilayered, highly interlocked stacking would be much preferred.[27,28] Unfortunately, GO is significantly affected by relative humidity because of its hydrophilic nature and is also affected by thermal shock, even at low temperatures, because of its structural metastability. As such, deposited thin-film GO layers should be chemically or thermally reduced to prevent water vapor transmission or water sorption on the surface. Another strategy is the preparation of graphene/polymer nanocomposites by the physical or chemical mixing of nanosheets or nanoplatelets of graphene and its derivatives [GO, rGO, and functionalized graphene oxide (FGO) or functionalized rGO] with polymers. Generally, to improve the gas-barrier properties of polymers, nonporous nanomaterials have been added to the polymer matrix as a filler to block gas or vapor diffusion. These nanofillers can increase the tortuosity, and this results in an extended travelling pathway of the diffusing gas through the polymer nanocomposites. To date, silicate clays with high aspect ratios (α) have been extensively investigated over the last decades because of their excellent barrier properties.[29–31]

The oxygen permeabilities of clay/polymer nanocomposites reported in the literature are summarized in Figure 1(d).[30,32–40] Despite their excellent gas-barrier properties, however, hydrophilic clay layers tend to aggregate easily because of their high face-to-face interaction stability due to van der Waals forces; they also tend to have face-to-edge interactions due to electrostatic forces[41] during mixing in solution.[42] As a result, such aggregation decrease the barrier properties of the resulting polymer nanocomposites. When compared with clays, graphene nanoplatelets have many advantages as 2D nanofiller materials for polymer nanocomposites in various aspects. Graphene-incorporated polymers show not only much enhanced gas-barrier properties but also reinforced mechanical strength and improved electrical conductivity and thermal properties when properly dispersed in a polymer matrix. As compared with other nanocarbons, such as carbon nanotubes (CNTs) and fullerenes, graphene has a higher surface-to-volume ratio and so will be able to achieve the longest gas-diffusion pathway, even at low volume factions. Also, GO can be well-dispersed with a high α, particularly in hydrophilic polymers.[43] In this article, we review the fundamental physical properties of graphene and its derivatives, focusing especially on barrier properties. The focus is primarily on the multilayer stacking of graphene and graphene/polymer nanocomposites for the practical use of the excellent barrier properties of graphene and its derivatives. Eventually, crucial factors that dominate gas-barrier performance in graphene/polymer nanocomposites are suggested, and theoretical predictions and experimental results are demonstrated on the basis of these factors.

GRAPHENE FOR BARRIER APPLICATIONS

Physical Properties of Graphene and its Synthesis

Since Novoselov et al.[44] reported monolayer graphene mechanically exfoliated from graphite, graphene has gained interest because of its many unique properties. Graphene is a single-atomic-layer honeycomb lattice of carbon atoms in a sp^2 hexagonal bonding configuration. It is a 2D allotrope of sp^2 carbon in the form of a planar monolayer. Compared with other nanomaterials, graphene is structurally unique, whereas the lateral dimensions of graphene are up to 10s of micrometers or larger, and the thickness is at the atomic scale. Graphene is known as the strongest material ever measured, with a Young's modulus of 1 TPa.[45] It exhibits a high thermal conductivity of 5300 W m^{-1} K^{-1} [46] and an extremely high surface area of 2630 m^2/g.[47] Moreover, graphene has a high electron mobility of 200,000 cm^2 V^{-1} s^{-1} [48] and an electrical conductivity of up to 1000 S/cm,[49] regardless of chirality, as in CNTs.[50]

To produce a large-area and defect-free graphene monolayer, many synthesis methods have been explored. Graphene can be synthesized by chemical vapor deposition (CVD) on metal substrates,[51,52] by epitaxial growth on SiC or metal substrates,[53,54] as graphene nanoribbons from unzipping CNTs,[55,56] from the mechanical cleavage of graphite,[44] and via the thermal and chemical reduction of GO.[49] Depending on the method, different types of graphene can be prepared in terms of scale, exfoliation degree, purity, and structural defects.[57] Among these methods, CVD growth method is mostly adapted to obtain high-quality graphene. However, graphene from a CVD method has many defects that may allow unfavorable molecular transport.[58–60] Early in CVD, grain boundaries between single-crystal graphene domains are formed by the connection of isolated graphene islands during growth. These grain boundaries in polycrystalline graphene dominate gas transport by unfavorable molecular transport.[58] Furthermore, graphene synthesized by the CVD method often causes intrinsic defects (1–15 nm in size); that is, it is difficult to prepare defect-free, perfect graphene.[60]

Gas-Impermeable Nature of Graphene

Graphene is known as a soft, 2D crystal material that is impermeable to any gaseous molecules, as demonstrated in molecular simulations[18,61] and experiments.[17] The electron density of aromatic rings in graphene is high enough to repel the penetration of atoms or molecules. For instance, when a monoatomic molecule, such as helium (He), approached the center of a carbon ring in a nondefective graphene monolayer, the energy barrier

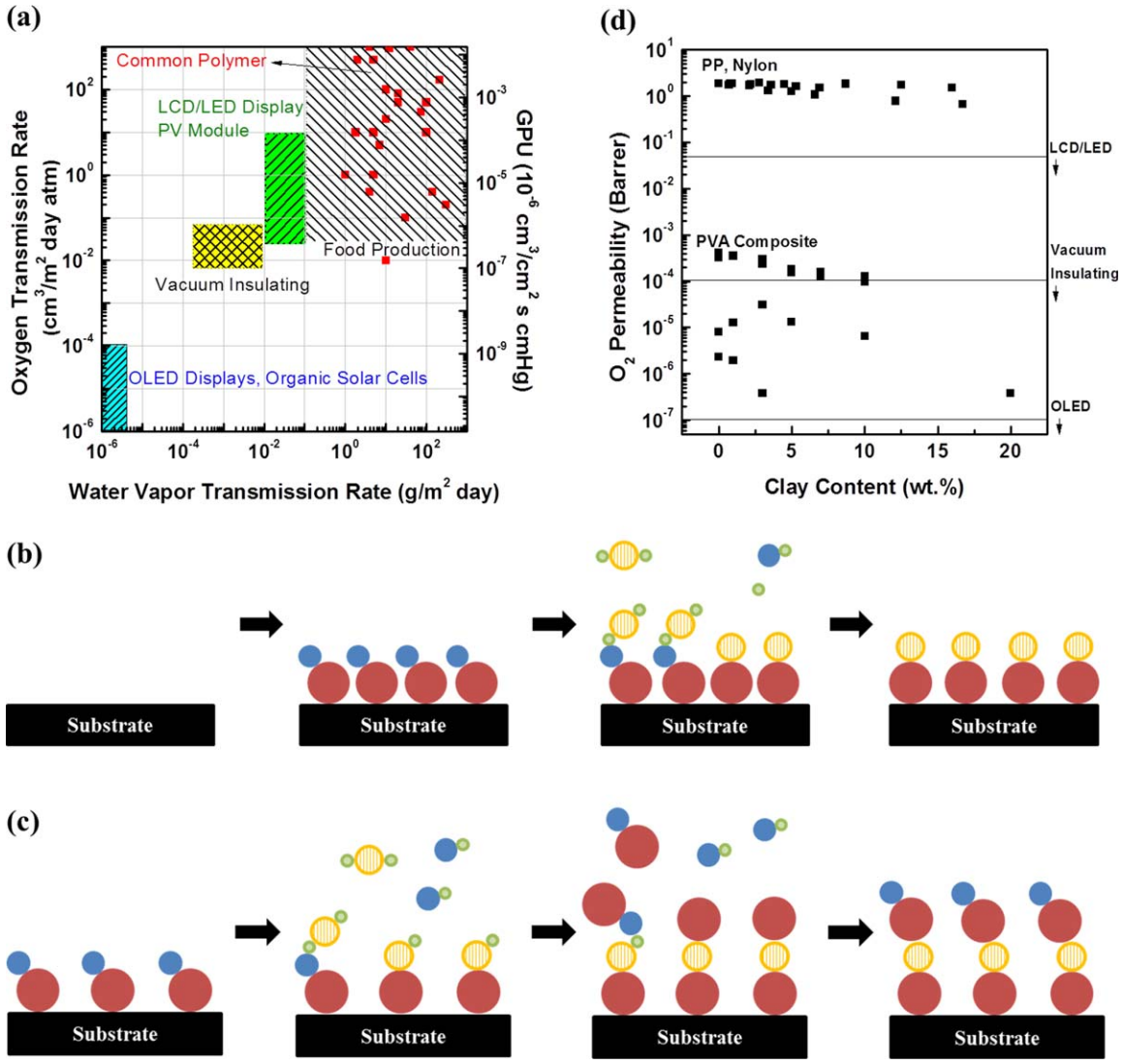

Figure 1. (a) OTR and WVTR of conventional polymeric barrier films and the requirements of gas-barrier films for various applications. (1 GPU (gas permeation unit)) = 10^{-6} cm^3 (STP) cm^{-2} s^{-1} $cmHg^{-1}$) (b,c) Schematic mechanisms of (b) ALD and (c) MLD. (d) Oxygen permeability of polymer/clay nanocomposites [1 Barrer = 10^{-10} cm^3 (STP) cm cm^{-2} s^{-1} $cmHg^{-1}$; LED = light-emitting diode]. [Color figure can be viewed in the online issue, which is available at wileyonlinelibrary.com.]

was calculated to be 18.8 eV[18] with local density approximation (LDA). The kinetic energy of the He atom (18.6 eV) was smaller than the energy barrier for penetration [18.8 eV; Figure 2(a)]. The relaxation of the graphene layer started only after the He atom was already reflected.[18] However, it is not easy to synthesize large-area, defect-free graphene sheets because there are some defects due to graphene boundaries, point defects, and carbon rings with more or less than six carbon atoms.[18] Figure 2(b) displays some examples of defective graphene models including Stone–Wales (SW) defects, and divacancies (555,777 and 858), tetravacancies, hexavacancies, and decavacancies. The energy barriers for these defects are 9.21, 8.77, 4.61, 1.20, 0.37, and 0.05 eV, respectively, as estimated by LDA.[18] The energy barrier heights of each defect are presented in Figure 2(c). Although the energy barrier decreases exponentially, they are still too high for an He atom to pass through a graphene plane ($k_BT = 26$ meV (k_B: Boltzmann constant, 1.38×10^{-23} J/K)]. Therefore, a defect-free, single-crystalline graphene monolayer can act as an excellent barrier against gas transport at room temperature. In addition, the pore diameter of the carbon ring in terms of the electron density is smaller than the kinetic diameter of various gases, that is, He (2.6 Å), H_2 (2.89 Å), CO_2 (3.3 Å), O_2 (3.46 Å), N_2 (3.64 Å), and CH_4 (3.8 Å). For example, the pore diameter of an octagon ring (considering electron density) is only 1.5 Å.[61] Only large vacancies with a size above 5 Å, that is, two lattice parameters, can be penetrated by gas molecules.[62,63] On the basis of the information presented previously, graphene is an excellent protective layer candidate when the graphene sheet can be successfully deposited onto polymeric substrates for gas-barrier applications.

Various Applications of Impermeable Graphene Sheets

For practical applications of graphene sheets, the preparation of large-area, defect-free graphene and a suitable method for

deposition onto polymeric substrates should be developed. Among the many preparation methods, epitaxial graphene growth on the SiC surface and the CVD growth of graphene on transition metals enable us to produce wafer-scaled monolayer graphene.[64] Freestanding graphene can also be prepared by the mechanical exfoliation of graphene on the microscale with etching,[65–67] photolithography from epitaxial growth,[68] and the CVD growth of graphene.[69,70] Some studies have involved the use of graphene as ideal molecular filters[71–73] and metal protecting layers to prevent the oxidation,[74–76] corrosion,[77,78] and degradation in electrochemical systems.[79] In addition, defective graphene can also be used for barrier film applications through the stacking of a number of graphene sheets.

Porous Graphene as an Ideal Molecular Filter. Graphene monolayers are impermeable to gaseous molecules and are suitable for protective barrier applications. However, if the pores could be properly engineered on a graphene plane, the subnanoporous graphene sheets could be used as a fast, selective molecular filter. The most ideal molecular filter should consist of an ultrathin layer for high throughput, regular and small pores for high gas selectivity, and high chemical and mechanical stability. Generally, porous graphene has been evaluated mainly with quantum mechanics and molecular dynamics simulations.[61,71,80] Jiang et al.[80] reported H_2/CH_4 separation with hydrogen-functionalized porous graphene with pore dimensions of 2.5 × 3.8 Å^2. The hydrogen-functionalized pores of 3.6 Å, which were larger than those of the octagon ring (1.5 Å) could weaken the π–π interaction near the pore; thus, a diffusion barrier for a large gaseous molecule, such as CH_4, was created.[61] They obtained a high H_2/CH_4 selectivity of 10^{23} at room temperature ($T = 300$ K). In addition, the H_2/N_2 and H_2/CO_2 selectivities of porous graphene were theoretically calculated to be 2 × 10^{12} and 1 × 10^{11}, respectively.[61] Recently, the separation of ^{3}He from ^{4}He with nitrogen-doped nanoporous graphene sheets was demonstrated with a molecular dynamics simulation.[81] Under the most ideal conditions, the maximum transmission ratio of ^{3}He/^{4}He reached 19 at $T = 10$ K.[71]

In addition to gas molecules, solvated ions passing through functionalized graphene (FG) nanopores and driven by an external electric field were also investigated with molecular dynamics.[82] It was revealed that monolayer graphene with nanopores could efficiently separate NaCl from water molecules, and the salt rejection strongly depended on the pore size, chemical functionalization, and transmembrane pressure. The predicted water permeability through the graphene membrane was three orders of magnitude higher than commercial reverse osmosis membranes. For example, the water permeability ranged from 30 to 66 L cm^{-2}·day^{-1}·MPa^{-1} with a hydrogenated pore diameter of 23.1 Å.[2,83] In addition, when a voltage was applied, the water molecules tended to be closely packed, showing a high water density near the graphene surface due to the polarization of water molecules.[84]

More recently, with the introduction of a water slab between a gas mixture and the graphene membrane, a specific gas could be separated on the basis of the water solubility of the gases, as shown in Figure 3(a).[85] That study demonstrated efficient CO_2

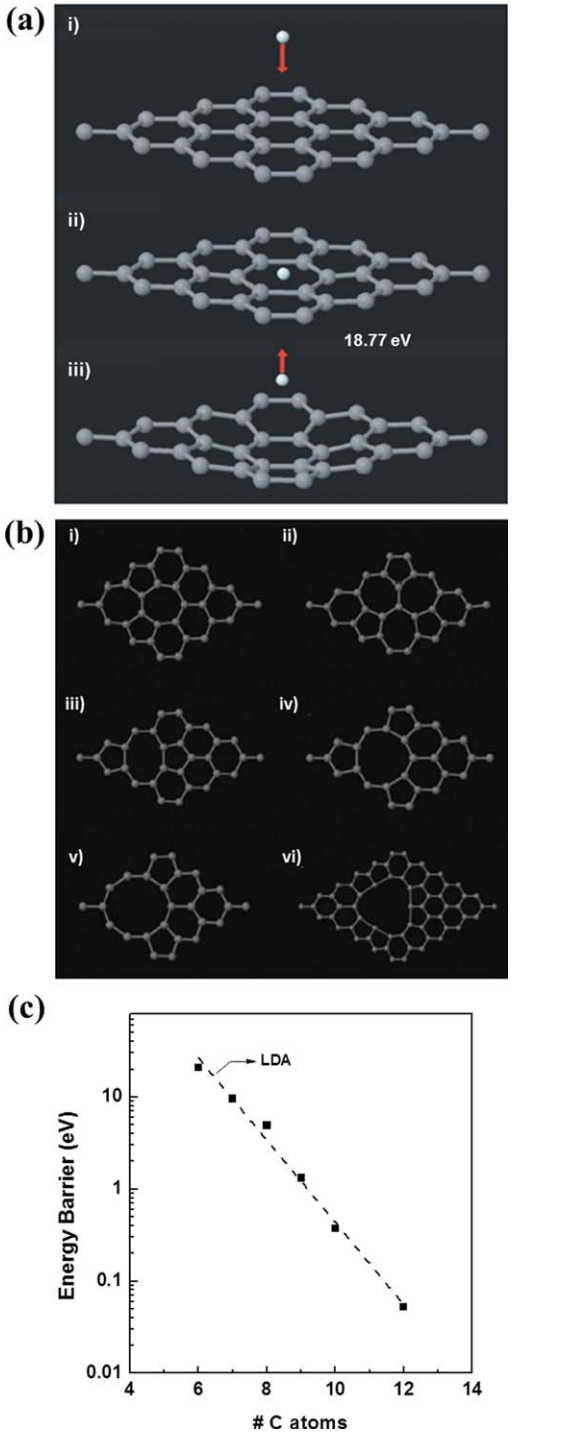

Figure 2. (a) Reflection of an He atom with a kinetic energy of 18.6 eV from a graphene surface: (i) The He atom approaches the perfect graphene layer. (ii) The He atom comes to rest before penetrating the graphene layer; the relaxation of the graphene layer is very small at this moment. (iii) The He atom is reflected back, and the surface starts to relax. (Reproduced with permission from ref. 17. Copyright 2008 ACS Publications.) (b) Defective graphene models: (i) SW defect, (ii) 555777 divacancy, (iii) 585 divacancy, (iv) tetravacancy, (v) hexavacancy, and (vi) decavacancy. (c) Dependence of the penetration energy barrier height on the size of the defect for LDA. (Reproduced with permission from ref. 17. Copyright 2008 ACS Publications.) [Color figure can be viewed in the online issue, which is available at wileyonlinelibrary.com.]

separation from CO_2/O_2, CO_2/N_2, and CO_2/CH_4 mixtures with a graphene pore size of 0.99 nm, and the selectivities reached 9.5, 14.4, and 9.9, respectively. However, the experimental approach to make such precise pore sizes on graphene would be a great challenge. At present, the pores can be generated with a focused electron beam of a transmission electron microscope;[86] however, there are some limitations in precision and resolution.

Protective Layers for Antioxidation Applications. Some studies have shown that graphene can also be used as a protective layer to prevent oxidation.[78,87] In general, to prevent refined metal corrosion, several methods have been proposed, including inert metal or alloy coating,[88,89] electroactive conducting polymer coating,[90] self-assembly monolayer coating,[91,92] and the formation of oxidized layers on the substrate surface.[93] However, these methods rely mainly on the physical properties of metals, such as optics, thickness, and electrical and thermal conductivity. When compared to these materials, graphene is chemically stable in an ambient atmosphere up to 400°C[94] and in an inert atmosphere up to 1500°C,[95] and it can be moved onto arbitrary surfaces by a transfer method. Chen et al.[87] showed the feasibility of graphene grown by CVD to protect a metal surface, such as Cu and Cu/Ni alloy, from oxidation and hydrogen peroxide. The uncoated Cu, monolayer graphene-coated Cu, and multilayer graphene-coated Cu were exposed to air at 200°C for the same periods of time. After 4 h, the graphene-coated Cu showed no significant surface changes, whereas the uncoated Cu became darker [Figure 3(b)]. Furthermore, CuO, Cu_2O, and $Cu(OH)_2$ were detected in the uncoated Cu. However, after 2 days, the monolayer graphene-coated Cu was also thermally oxidized to some extent. Indeed, graphene without defects and grain boundaries may have been able to preserve the metal surface under reactive environments over a long period because of its perfect barrier properties. However, polycrystalline graphene grown by CVD contained defective grain boundaries and some defects that could have allowed the penetration of oxidants into the metal surface on the bottom. Graphene-coated Cu also exhibited an excellent tolerance against electrochemical corrosion[87] by hindering electrolytes approaching the corroded electrode area.[78] Electrochemical corrosion was also observed at the grain boundaries of polycrystalline graphene. Molecular diffusion through defective grain boundaries would be a crucial factor for the development of effective oxidation protection. To make more protective films with graphene, less defective and large-grain-sized graphene should be developed with more the stable physical transfer of graphene sheets on the desired substrates.

Few-Layered Graphene on Polymeric Substrates. One of the simple strategies in the use of defective graphene as a gas-barrier film is the multistacking of graphene layers. For example, few-layered graphene can be transferred onto a polymeric substrate such as poly(1-methylsilyl-1-propyne) (PTMSP) films [Figure 3(c)]. PTMSP is a highly permeable, rigid, glassy polymer,[96] which is expected to provide a rapid indication of the effect of graphene layers on the gas-barrier properties. The gas molecules can enter through grain boundaries or defects on the graphene layer. However, the gas permeabilities are reduced by an increase in the number of graphene layers, as shown in Figure 3(d). In addition, gas selectivities increase over typical polymeric membranes[97] and carbon molecular-sieve membranes.[98] This implies that the molecular sieving mechanism may occur between graphene interlayers. This phenomenon shows that single-layer graphene can act as a gas-barrier material, as suggested theoretically; however, gas can still diffuse through multilayer graphene because of transfer-induced macroscopic holes and grain boundary defects in the graphene sheets. Therefore, to use graphene as a gas-barrier material in practical applications, graphene grown on copper foils should be single crystal, have less structural disorder, and also have reduced macroscopic defects during transfer to polymeric substrates.

In general, graphene grown by CVD has a polycrystalline phase, point defects, and nanoscale large holes. Other defects are often formed during the transfer process from the metal to any desirable substrates.[60] One common method for transferring graphene from a transition metal growth substrate is the so-called poly(methyl methacrylate) (PMMA)-mediated transfer.[99–101] Once PMMA is coated onto a graphene surface, the metal under graphene is etched by oxidative etchants such as $FeCl_3$. Then, a freestanding graphene/PMMA film is transferred onto the target substrate, and the PMMA layer is removed with acetone. This method is quite simple; however, the formation of undesirable defects is unavoidable during the transfer process, also, PMMA residues remain as minor impurities.[100] In addition, the graphene quality after transfer is influenced largely by the surface nature (hydrophilicity or hydrophobicity) of the substrate, the surface roughness of copper, and the type of etchant used to remove the copper. To minimize defects and obtain high-quality graphene, many studies have been reported; these include spin-coating, the preannealing of the copper substrate before CVD,[102] the annealing of the graphene/copper layer,[103] SiO_2 growth on graphene followed by back etching,[104] and etchant and temperature control.

There have been many studies based on theoretical approaches on the preparation of high-quality graphene without defects on a large scale. However, there are still many prerequisites to the synthesis of perfect graphene with theoretically ideal properties because of the limitation of recent techniques. Therefore, in the future, techniques for growing perfect graphene, nondefective transfer methods, nanopore tuning with advanced electron-beam resolution, and easy multilayer stacking techniques need to be developed.

GO FOR BARRIER APPLICATIONS

Synthesis and Properties of GO

Although the micromechanical exfoliation, CVD, and epitaxial growth of graphene are suitable for producing high-quality graphene, they have some technical limitations that may not be applied to scaled-up graphene production.[57] Moreover, graphene itself has a low processability with conventional polymers and solvents in chemical processes. In contrast, the chemical oxidation of graphite in solution as a precursor of graphene is easy to scale-up in bulk, and chemically oxidized graphite itself has a higher processability. The oxidation of graphite to GO dates back to 1859, when Brodie[105] used fuming nitric acid and

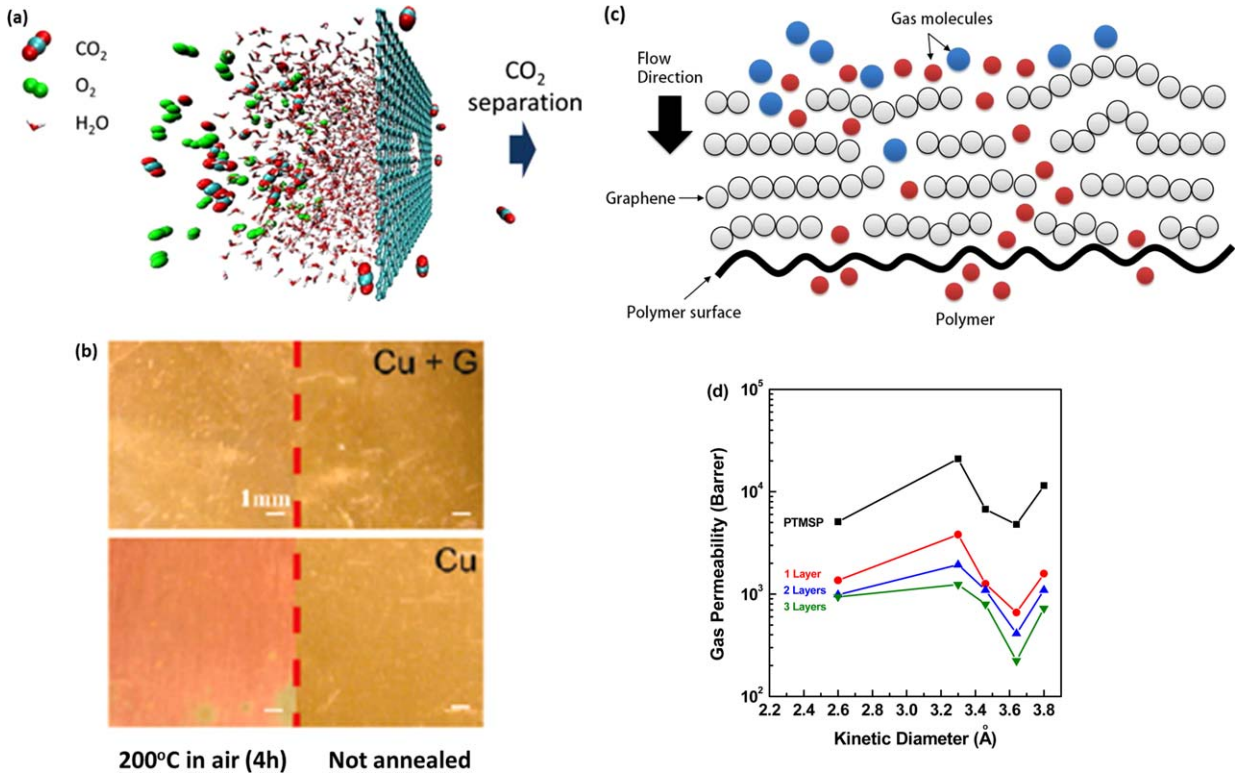

Figure 3. (a) Illustration of the water-solubility-driven separation of CO_2 with porous graphene. (Reproduced with permission from ref. 84. Copyright 2012 Elsevier, Ltd.). (b) Photographs of Cu and Cu/Ni foil with and without a graphene coating taken before and after annealing in air at 200°C for 4 h. (Reproduced with permission from ref. 86. Copyright 2008 ACS Publications.) (c) Illustration of the gas-transport mechanism in multilayer graphene-deposited polymer film. The gas can penetrate the defective pores in graphene sheet. (d) Change in gas permeability as a function of the number of graphene sheet on polymer film. [Color figure can be viewed in the online issue, which is available at wileyonlinelibrary.com.]

potassium chlorate ($KClO_3$) to oxidize graphite. A century later, Hummers and Offeman[106] proposed a new synthesis method for the oxidation of graphite with potassium permanganate ($KMnO_4$) and concentrated sulfuric acid as oxidizing agents. After these pioneering studies, the Hummers method and its modified methods have been widely adapted for synthesizing GO. Commonly used GO synthesis methods are summarized in Table I. GO consists of oxygen functional groups on the basal plane and at the edges, as proposed by Lerf and coworkers.[107,108] In most cases, it is believed that epoxy and hydroxyl groups are on the basal plane, whereas carbonyl and carboxylic acid groups are at the edges.[109–113] However, the exact chemical structure of GO is still being explored. When compared to graphene, the oxygen functional groups in GO result in some structural defects.[114,115] However, carboxylic acid groups at the edges help to electrostatically stabilize the colloidal state of a GO suspension in some polar solvents, particularly in water at high pH without any surfactant.[116,117] To achieve a fully exfoliated GO suspension, posttreatments such as ultrasonication[118] and further centrifugation[119] may be needed. The monolayer thickness of GO is known to be about 1–1.4 nm[120,121] thicker than that of monolayer graphene (0.34 nm)[122] because of oxygen-containing functional groups on the basal plane.

GO can be a precursor of graphene via chemical or thermal reduction methods. Oxygen-containing functional groups in GO are mostly eliminated by reduction processes, and then, the electrical and thermal conductivities of rGO return to being close to those of graphene. In general, there are various reduction methods, such as high-temperature thermal reduction,[123] low-temperature chemical reduction,[124] and irradiation-assisted reduction.[125] Thermal reduction is usually performed above 200°C *in vacuo*[126] and in an inert atmosphere.[127] Typically, a more efficient reduction can be achieved at high temperatures because some oxygen functional groups can gradually decompose at temperatures above 200°C.[128] Chemical reduction can also be achieved in both the liquid and gas phases. Chemical reducing agents include hydrazine,[128–130] metal hydrides (e.g., NaH[131] and $NaBH_4$[132]), ascorbic acid (Vitamin C),[133] Hydrogen Iodide (HI) gas,[134] hydroquinone,[135] and *p*-phenylenediamine.[136] GO reduction can also be achieved at high temperature and with strong alkaline treatment (KOH and NaOH)[137] or in supercritical water.[138] In addition, UV-assisted photocatalytic reduction[125] and microwave-assisted reduction[139,140] are also used for GO reduction. A multistep reduction based on a combination of different processes is also an effective route for removing oxygen-containing functional groups.[141] However, none of the reported reduction methods have ever achieved the complete removal of oxygen groups and have achieved only a partial restoration of an sp^2-conjugated graphene network.[142,143] In addition, rGO has many defects on its basal plane. Thermal

Table I. Summary of GO Synthesis Methods

Method	Oxidants	Solvent	Oxidation time	C/O ratio	Advantages	Drawbacks	Reference
Brodie	$KClO_3$	HNO_3	3–4 days	2.16	Very stable, low contamination, small interlayer distance	Slow	105
Modified Brodie	$NaClO_3$	HNO_3	1–2 days	2.47–2.64			229
	$NaClO_3$	HNO_3	1.5 days	2.04			230
Staudenmaier	$KClO_3$	HNO_3, H_2SO_4	4 days	2.6			234
Hummers	$NaNO_3$, $KMnO_4$	H_2SO_4	1 h	2.25	Fast reaction Fewer defects	High contamination and degradation	235
Modified Hummers	$K_2S_2O_8$, P_2O_5, $KMnO_4$	H_2SO_4	8 h	1.3			236
	$KMnO_4$	H_2SO_4, H_3PO_4	19 h	—			237

reduction processes cause vacancies in the basal plane because of the evolution of carbon in the form of CO or CO_2.[144] Chemical reduction with reducing agents also forms defects on the rGO surface and a layering structure and can cause additional doping on defective sites.

Preparation of Thin GO Films

With the use of a well-dispersed GO solution, it is possible to prepare thin GO films on various substrates. Thin GO films and thick GO papers have interlocked layered structures of 2D GO sheets.[145] This layered structure leads to a great mechanical strength and flexibility, even for films with submicrometer thicknesses.[146] Thin GO films can be prepared with the Langmuir–Blodgett,[112,147] drop-casting,[148] dip-coating,[127] spraying,[149,150] electrophoresis,[136,151] vacuum-filtration,[145,152] and spin-coating methods.[111,153–155] Once GO is assembled in a multilayer, strong hydrogen bonds between individual GO sheets hold the sheets together to maintain interlocked, layered structures. Thus, such GO films show an elastic modulus of 207.6 GPa,[43] which is lower than that of graphene but still high. In addition, more stable and thin GO films can also be prepared on hydrophilic substrates.

Among the many methods, drop casting, dip coating, and spray coating often result in nonuniform deposition, which is caused by self-aggregation. On the other hand, the spin-coating method results in a homogeneous GO film [Figure 4(a)]. Therein, to obtain a uniform GO film, inert gas is blown to the center of the substrates to accelerate rapid vaporization of solvent.[25] The film thickness can be controlled via the adjustment of the GO concentration or coating cycles.

The vacuum-filtration method has been commonly used for the preparation of thin GO films on substrates or freestanding, thick GO papers [Figure 4(b)]. As the GO suspension is filtered through porous substrates, GO nanosheets are continuously stacked on the porous substrate. This process enables a nanoscale thick GO film via the adjustment of the amount of filtered GO suspensions.

Other self-assembly processes at liquid–air[26,156] or liquid–liquid interfaces[157,158] have also been used to prepare ultrathin assemblies of GO thin films. Because GO is regarded as an amphiphilic soft material, GO films can be prepared between aqueous and nonaqueous liquid interfaces[111] and thereby potentially reduce the structural defects.[159] As shown in Figure 4(c), layer-by-layer (LBL) self-assembly on polymers is a useful method for preparing barrier GO/polymer films.[160] Using LBL self-assembly, nanometer thick GO layers can be achieved by the adsorption of oppositely charged polyelectrolytes on a polymeric substrate. GO has negative charges on the surfaces; therefore, GO can be used to form a thin barrier film with polycations with LBL deposition; these LBL structures show excellent gas-barrier properties.[161]

Gas-Transport Model in Multilayered GO Films

Figure 4(d) shows transmission electron microscopy images of GO layered structures on a polymer substrate. A simple gas permeability model for a regular arrangement of platelets was proposed by Nielsen [Figure 4(e)] for the case where gas molecules pass through the layer structure in the perpendicular direction.[162] These layered structures maximize the gas-diffusion path length and, as a result, significantly decrease the gas flux through layered composite films. The diffusion length (l') can be estimated as follows:[163]

$$l' = l + \langle N \rangle \frac{L}{2} \quad (1)$$

$$\langle N \rangle = \frac{l}{D' + W} \quad (2)$$

where l is the membrane thickness, L is the width of the graphene sheet, D' is the effective distance between graphene

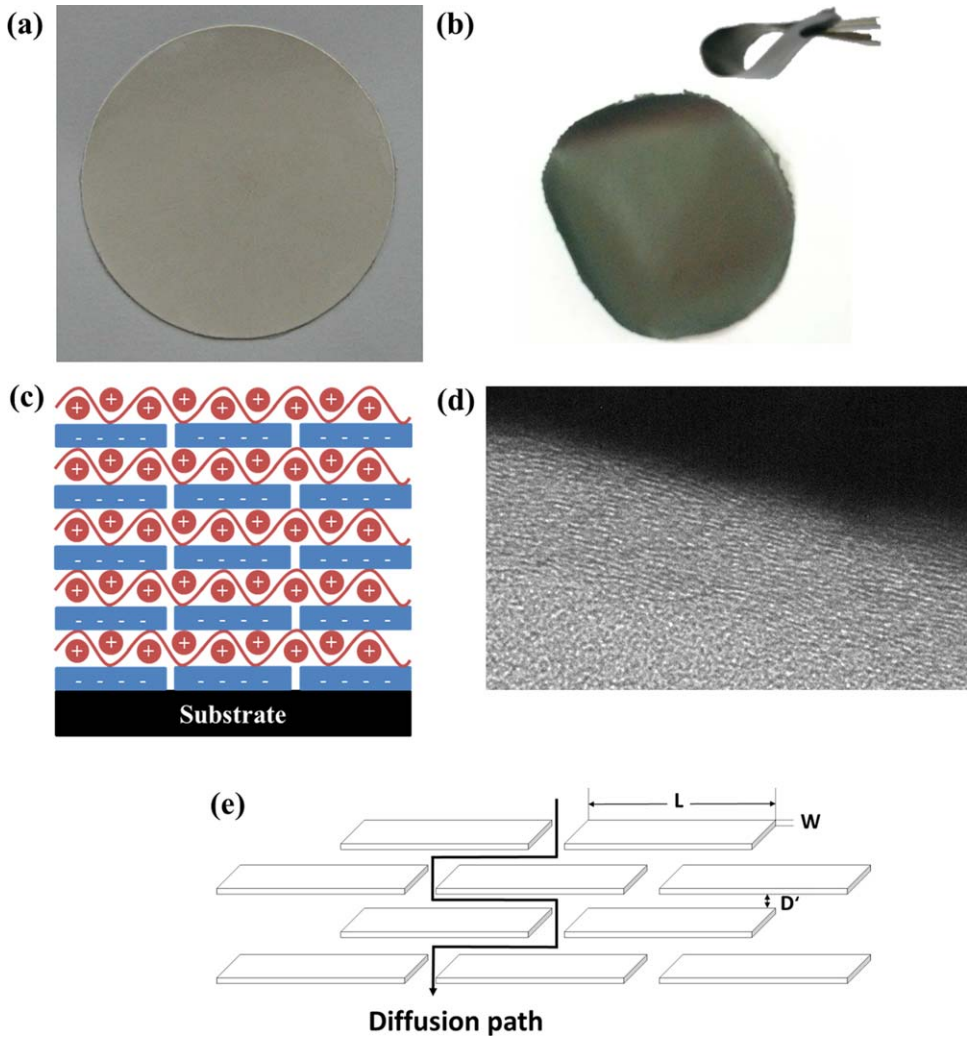

Figure 4. (a) GO thin film on microporous polymer membranes prepared by spin-coating. (b) Freestanding GO film prepared by vacuum filtration. (c) LBL structure of a GO/polycation composite film (the blue and negatively charged platelet is GO, and the red and positively charged chain is the polycation). (d) Cross-sectional TEM image of GO prepared by spin-coating on polymer substrate. (e) Regular arrangement of horizontally stacked platelets in a parallel array perpendicular to the diffusion direction. [Color figure can be viewed in the online issue, which is available at wileyonlinelibrary.com.]

sheets,[133,164,165] and W is the thickness of the graphene sheet.[121] GO is supposed to be rectangular in shape and oriented perpendicular to the direction of gas diffusion; therefore, GO acts as a perfectly impermeable barrier against gas diffusion. The diffusional path length in layered GO paper is significantly influenced by the GO platelet size. For large platelet sizes of 5 μm, the diffusional path is 1300 times longer than the membrane thickness. On the other hand, for a small GO platelet size of 100 nm, the diffusion path is only 25 times longer than the membrane thickness. Therefore, for barrier applications, large GO platelet sizes are preferred over small GO platelet sizes.

Barrier Applications of GO Films

Gas Barrier. Freestanding GO films in a dry state do not allow even small gas molecules such as He to penetrate through the GO sheets because of a high potential energy barrier. Therefore, if the gas molecules are to permeate through the GO film, the gas molecules must enter the boundaries between the top layers of GO films and then pass along the interlayer space with a long, tortuous path.[166] Thus, the tortuosity is influenced by the GO platelet size and thickness, whereas stacking structures and residual water content are also significant in the improvement of the gas-barrier properties of GO films. Figure 5(a) shows the gas permeability of thick GO films with different platelet sizes. The maximum size of a GO platelet is dependent on the size of the initial graphite source.[148] In addition, the average size of GO platelets can be controlled on the nanoscale by the extension of the oxidation[167] or ultrasonication time.[168] In Figure 5(a), the gas transport through different platelet sizes of GO films shows molecular sieving behavior, and the gas permeabilities increase as the sonication time increases because the average GO platelet size becomes smaller. For example, a GO film prepared from a smaller GO platelet size shows a much higher gas permeability because of fewer diffusional pathways of gas molecules. Figure 5(b) shows He permeance through GO films as a function of applied feed pressure (the permeate side is at

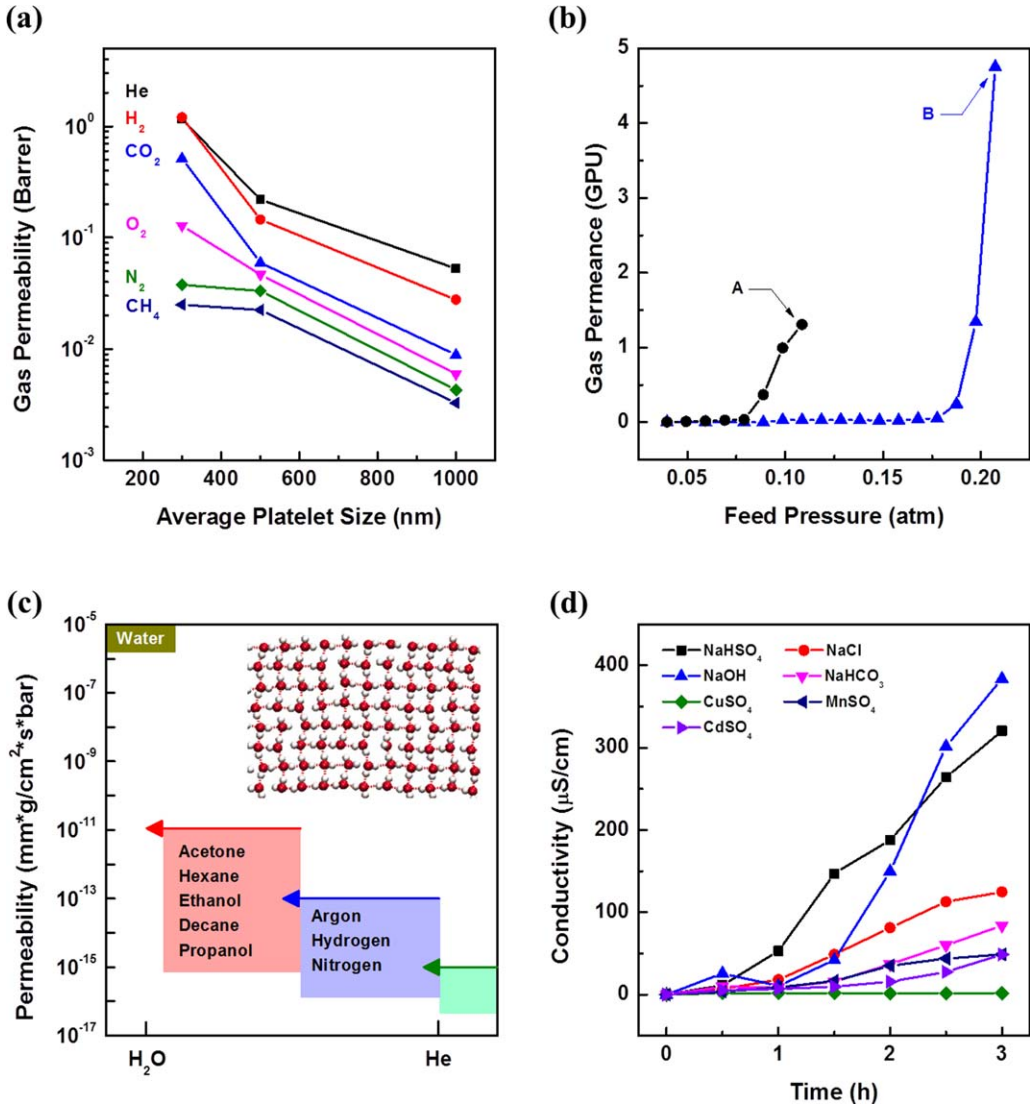

Figure 5. (a) Gas permeability of thick GO films with different platelet sizes. (b) He permeance of ultrathin GO films as a function of feed pressure. (Average platelet size of A: 3 μm, B: 1 μm) (c) Permeability of GO paper with respect to water and various small molecules. (1GPU = 10^{-6} cm^3 (STP) cm^{-2} $s^{-1}cmHg^{-1}$) (Reproduced with permission from ref. 172. Copyright 2012 American Association for the Advancement of Science.) (d) Conductivities of different ionic compounds through GO membranes. (Reproduced with permission from ref. 27. Copyright 2013 ACS Publications). [Color figure can be viewed in the online issue, which is available at wileyonlinelibrary.com.]

atmospheric pressure). At low feed pressures, a gas molecule could not enter the GO interlayer space because the kinetic energy of the gas molecule is smaller than the potential energy barrier of the GO sheets. However, as the applied pressure is increased, the gas molecules can permeate through the interlayer space of GO because the kinetic energy of the gas starts to overcome the potential energy barrier of the GO sheets. Furthermore, as the GO platelet size increases, the total potential energy barrier of the GO sheets will be higher; therefore, a high feed pressure will be needed to provide a high kinetic energy to the gas molecules to overcome the potential energy barrier of the GO sheets. In addition, humidity is also a critical issue because the hydrophilic functional groups of GO can bind with water molecules. Then, not only the distance between GO layers, which is strongly dependent on the water content of the GO sheets (due to the humidity in ambient conditions)[169] but also the interaction between gas and water molecules should be considered.

Selective Ion Transport. Unlike graphene, some studies have successfully demonstrated GO membranes as ion-selective membranes.[27,170,171] As shown in Figure 5(c), water molecules can permeate through the interlayer spaces between GO sheets, whereas other liquids and gases are blocked.[172] Sun et al.[27] showed the selective ion transport and water purification properties of freestanding GO membranes prepared by a drop-casting method. Sodium salts permeated quickly through the GO membranes, whereas heavy-metal salts, such as Mn^{2+}, Cu^{2+}, and Cd^{2+} salts, moved much more slowly, as presented in Figure 5(d). Heavy-metal salts were rejected because of their

strong interactions with the GO functional groups.[170] Furthermore, the oxygen-functional-group-decorated GO sheets maintained a relatively large interlayer distance and provided empty spaces between nonoxidized regions.

GO films provide good barrier properties in the dry state; however, the interlayer distance between GO sheets, which significantly affects the gas molecular transport, is very susceptible to humidity. There are two strategies for overcoming the humidity problem: the complete elimination of water and the elimination of the oxygen groups of GO. The complete elimination of water is ideal, but it is still hard to achieve because of the thermal and structural properties of GO. However, through the control of the humidity, the gas or ion selectivity of a GO film can be adjusted. To eliminate oxygen groups in GO, various reduction treatments should be performed. However, rGO films do not form well-ordered layering structures because of the deformation of GO sheets during the reduction process. To ensure the mechanical strength of the GO film, a sufficiently thick GO film is needed. Fortunately, additional chemical crosslinking can be conducted to enhance the mechanical properties between the oxygen groups of GO and divalent ions[170] or other crosslinkers, such as polyallylamine.[173] Therefore, the functionalization of GO to enhance the mechanical properties and vapor stability and a complete reduction method of GO without structural defects should be developed for the use of GO for barrier applications.

GRAPHENE/POLYMER NANOCOMPOSITES

Gas-Diffusion Barrier

There is a strong demand for improving the gas-barrier properties of existing polymers used in electronic devices and food packaging, which require the near-perfect exclusion of gas molecules. The fabrication of polymer nanocomposites, which are intended to provide a synergetic effect by taking advantage of the high workability of both polymers and functional fillers, is a useful method for overcoming the limits of the physical properties of the polymers themselves.[174] Since Toyota Co.[29] showed excellent improvement in the mechanical strength of nylon 6 by adding clay to form polymer nanocomposites 20 years ago, polymer nanocomposites have been investigated extensively for many technical applications. In particular, the incorporation of nanoscale fillers leads to the enhancement of many properties, even with lower loading amounts than microscale fillers.[175] Among the many kinds of nanofillers, silicate clays are widely used for barrier applications because of their high α and their compatibility with various polymers.[176–179] However, as mentioned earlier, the aggregation of clays and their small lateral size still limit the wide use of clays as a fillers for polymer nanocomposites.[180] To overcome these disadvantages of clay nanofillers, a number of modification methods have been suggested.[181–186] Recently, graphene and its derivatives have come to be regarded as promising 2D layered nanofillers.[187,188] Graphene provides not only a high α but also useful physical properties, such as a high electron mobility, thermal conductivity, mechanical properties, and optical transmittance.[46,57,189–191] Because of these unique properties, graphene can contribute to higher performance in polymer nanocomposites.[192]

Preparation Methods of Graphene/Polymer Nanocomposites

Graphene/polymer nanocomposites mentioned in the literature are summarized in terms of their target properties, polymers, type of graphene, and preparation methods in Table II. In general, the incorporation of graphene and its derivatives into polymers are mainly done to reinforce the mechanical strength, enhance the electrical conductivity, and impart gas-barrier properties. Depending on the applications of nanocomposites, different polymer matrices and types of graphene fillers can be selected with various compositions. Polymer nanocomposites are prepared mostly by solution mixing, *in situ* polymerization, and melting.[193]

The solution-mixing method is widely used because of the facile nature of the process.[194] The crucial challenges in solution mixing are minimizing the residual solvents[195] and obtaining good dispersion properties of the fillers in viscous polymeric solutions. Complete drying to eliminate residual solvents is needed; however, in the case of GO as a nanofiller, the thermal reduction of GO should be carefully considered because GO can easily decompose, even at low temperatures below 150°C; this often leads to local structural deformations in the polymer matrix, which causes a significant loss of the physical properties in the resulting graphene/polymer nanocomposites. The composition of graphene nanoplatelets is also significantly affected by the degree of dispersion in the mixing solution. Furthermore, aggregated graphene or GO nanoplatelets, because of the poor solubility or gravimetric precipitation by unexfoliated graphene or GO nanosheets, is a critical problem often occurring in such nanocomposites.[196] However, the solution-mixing method is a convenient method when residual solvents can be eliminated completely and an excellent dispersion can be achieved.[194]

In situ polymerization is another route for preparing homogeneously dispersed graphene or GO nanoplatelets in a polymer matrix because of the interactions forming chemical bonds between the graphene derivatives and the polymer matrix.[194,197] In addition, through the induction of additional functional groups on the graphene or GO surfaces, *in situ* polymerizations can provide enhanced dispersion properties and also better compatibility between graphene and the polymer via chemical bonding. Fine powders or uniformly dispersed graphene nanoplatelets in solvent can be mixed with a monomer solution with an initiator (e.g., photoinitiators and thermal initiators). After the initiator is dissociated by radiation or thermal energy, exfoliated graphene or GO nanoplatelets can be mixed or crosslinked with polymer chains; this leads to higher dispersion properties. During polymerization, however, the viscosity usually increases, which may reduce the processability of nanocomposites.[192,195] Moreover, *in situ* polymerization should also be performed in the solution state; therefore, the elimination of residual solvents should be addressed when one uses the solution-mixing method.[197]

Melt processing is a typical method for the preparation of thermoplastic polymer nanocomposites.[197] It is an ecofriendly, cheap, and suitable method for mass production in industrial applications.[192,198] In general, graphene or GO powders can be blended with polymers. The polymers are heated until they are in a molten

Table II. Preparation of the Graphene/Polymer Nanocomposites

Polymer	Types of graphene	Preparation method[a]	Maximum fraction	Reference
Mechanical strength				
PU	rGO, FGO	Blending, *in situ*, melting	3 wt %	238
PI	FGO	*In situ*	0.38 wt %	239
PAN	EG	*In situ*	4 wt %	223
PLA	EG	Melting	7 wt %	240
WPU	FG	Solution mixing	6 wt %	241
PPS	EG	Melting	25 wt %	242
PI	GO	*In situ*	5 wt %	243
PVE	rGO	*In situ*	0.2 wt %	244
PMMA	GO	Solution mixing	10 wt %	245
PC	Graphite, FG	Melting	15 (G), 3 (FG, wt % %)	213
Cellulose	G	Solution mixing	5 wt %	219
PEN	Graphite, EG	Melting	20 (G), 4 (EG, wt % %)	246
LLDPE	FG	Solution mixing	5 wt %	230
Poly(norbornene dicarboximide)	FG	Solution mixing	5 wt %	247
PET	FGO	Solution mixing	3 wt %	220
PLA	GO, graphene	Solution mixing	0.6 wt %	218
Butadiene–styrene–vinyl pyridine rubber	GO	Melting	3.6 vol %	248
PET	rGO	Melting	1.5 wt %	222
PVA	GO	Solution mixing	5 wt %	249
HDPE	FGO	Melting	0.6 wt %	250
Cellulose	GO	Solution mixing	7.5 wt %	251
PU	GO	*In situ*	4.4 wt %	252
PS	GO	Solution mixing	3 wt %	253
PAH, PSS	GO	LBL	8 vol %	254
PVA	GO	Solution mixing	0.7 wt %	255
Poly(allylamine hydrochloride)	GO	*In situ*	12.5 wt %	256
PS	FG	*In situ*	0.9 wt %	257
Epoxy	rGO	Solution mixing	0.1 wt %	258
PMMA	GO	Grafting	3 wt %	259
Nylon 6	G	*In situ*	10 wt %	57
PU	rGO	*In situ*	2 wt %	260
PI	GO	*In situ*	5 wt %	261
PVA	rGO	Solution mixing	3 vol %	262
PVA	GO, rGO	Solution mixing	4 wt %	263
PVA	rGO	Solution mixing	3.5 wt %	264
PMMA	GO, rGO	*In situ*	0.05 wt %	265
PVDF	GO	Solution mixing	2 wt %	266
SAN, PC, PP, PA	rGO	Melting	12 wt %	267
PU	rGO	*In situ*	2 wt %	260

TABLE II. *Continued*

Polymer	Types of graphene	Preparation method[a]	Maximum fraction	Reference
PVC	rGO	Solution mixing	2 wt %	268
PP	EG	Melting	25 vol %	269
PCL	GO, graphite	Solution mixing	10 wt %	270
Electrical conductivity				
PBI	GO, FGO	Mixing	2 wt %	271
PS	G	Mixing	20 wt %	272
PVC-*co*-PVA	rGO, EG	Solution mixing	0.7 vol %	273
PEId, epoxy	EG	Soaking	0.79 wt %	274
PU	rGO, FGO	Blending, *in situ*, melting	3 wt %	238
PAA	GO	LBL	13 layers	275
PANI	GO	*In situ*	10 wt %	276
PMMA	EG	*In situ*	0.31 vol %	277
PI	FGO	*In situ*	0.38 wt %	239
PAH	GO	LBL	4 Layer	236
PAN	EG	*In situ*	4 wt %	223
PLA	EG	Melting	7 wt %	240
PS	FG	Solution mixing	10 vol %	168
PPS	EG	Melting	25 wt %	242
PVE	rGO	*In situ*	0.2 wt %	244
PEN	Graphite, EG	Melting	20 (G), 4 (EG, wt %)	246
PANI	FG	*In situ*	0.5 wt %	224
PU	rGO	*In situ*	2 wt %	260
SAN, PC, PP, PA	rGO	Melting	12 wt %	267
PU	rGO	*In situ*	2 wt %	260
Gas-barrier properties				
PEId, epoxy	EG	Soaking	0.79 wt %	274
PU	rGO, FGO	Blending, *in situ*, melting	3 wt %	238
PAN	EG	*In situ*	4 wt %	223
PVA	GO, rGO	Solution mixing	0.3 vol %	220
PVA	GO	*In situ*	0.72 vol %	278
PS	GO	Melting	2.27 vol %	279
PMMA	GO	Solution mixing	10 wt %	245
PI	GO	Solution mixing	0.01 wt %	280
PC	Graphite, FG	Melting	15 (G), 3 (FG, wt %)	213
PEI	GO	LBL	0.2 wt %	281
Cellulose	G	Solution mixing	5 wt %	219
PEN	Graphite, EG	Melting	20 (G), 4 (EG, wt %)	246
PEI	GO	LBL	0.5 wt %	282
LLPDE	FG	Solution mixing	5 wt %	230

TABLE II. *Continued*

Polymer	Types of graphene	Preparation method[a]	Maximum fraction	Reference
Poly(norbornene dicarboximide)	FG	Solution mixing	5 wt %	61
PET	FGO	Solution mixing	3 wt %	221
PLA	GO, graphene	Solution mixing	0.6 wt %	218
Butadiene–styrene–vinyl pyridine rubber	GO	Melting	3.6 vol %	248
PP	rGO	Melting	1 wt %	226
PANI	FG	*In situ*	0.5 wt %	224
PET	rGO	Melting	1.5 wt %	222
Thermal stability				
PS	G	Mixing	20 wt %	272
PEId, Epoxy	EG	Soaking	0.79 wt %	274
PAN, PAA, PMMA	EG, FG	Solution mixing	1 wt %	283
PPy	rGO	*In situ*	20 wt %	284
PLA	EG	Melting	7 wt %	240
WPU	FG	Solution mixing	6 wt %	241
PVE	rGO	*In situ*	0.2 wt %	244
Epoxy	G, GO, FGO	*In situ*	5 wt %	285
PI	GO	Solution mixing	0.01 wt %	280
PC	Graphite, FG	Melting	15 (G), 3 (FG, wt %)	213
PEN	Graphite, EG	Melting	20 (G), 4 (EG, wt %)	246
LLPDE	FG	Solution mixing	5 wt %	230
PP	rGO	Melting	1 wt %	226
PET	rGO	Melting	1.5 wt %	222
HDPE	FGO	Melting	0.6 wt %	250
Cellulose	GO	Solution mixing	7.5 wt %	251
PS	FG	*In situ*	0.9 wt %	257
Nylon 6	G	*In situ*	10 wt %	57
PU	rGO	*In situ*	2 wt %	260
PVA	GO, rGO	Solution mixing	4 wt %	263
PVDF	GO	Solution mixing	2 wt %	266
PU	rGO	*In situ*	2 wt %	260
Epoxy	rGO	Solution mixing	20 vol %	286
PVC	rGO	Solution mixing	2 wt %	268
PP	EG	Melting	25 vol %	269
PCL	GO, graphite	Solution mixing	10 wt %	270

[a] *In situ* in this column refers to *in situ* polymerization.
PAN: Polyacrylonitrile, PU: Polyurethane, WPU: Waterborne polyurethane, PVE: Polyvinyl ether, PC: Polycarbonate, PCL: Polycaprolactone, PEN: Polyethylene naphthalate, PS: Polystyrene, PSS: Polystyrene sulfonate, PAH: Polyallylamine hydrochloride, LLPDE: Linear low-density polyethylene, HDPE: High-density polyethylene, PA: Polyamide, PVDF: Polyvinylidene fluoride, SAN: Styrene Acrylonitrile, PBI: Polybenzimidazole, PEId: Polyetherimide, PPS: Polyphenylene sulfide, PAA: Polyacrylic acid.
"G" in the column of "Types of graphene" means graphene.
"G" in the column of "Maximum fraction" means graphite.

state, and then, the mechanically blended molten compounds are extruded. In the melting process, no solvent is necessary,[198] making it is an economical and environmentally friendly method suitable for scale-up.[176] However, in this process, strong shear forces are required to blend the highly viscous molten polymers and graphene derivatives. Here, graphene buckling, which causes rolling or shortening of the graphene derivatives, may occur. The reduction of α in graphene derivatives may not be suitable for achieving high conductivity in the resulting polymer nanocomposites,[197,198] whereas the high α is one of the best advantages over typical clays or other nanofillers. In addition to these common methods, the solid-state intercalation,[199] emulsion,[200] supercritical carbon

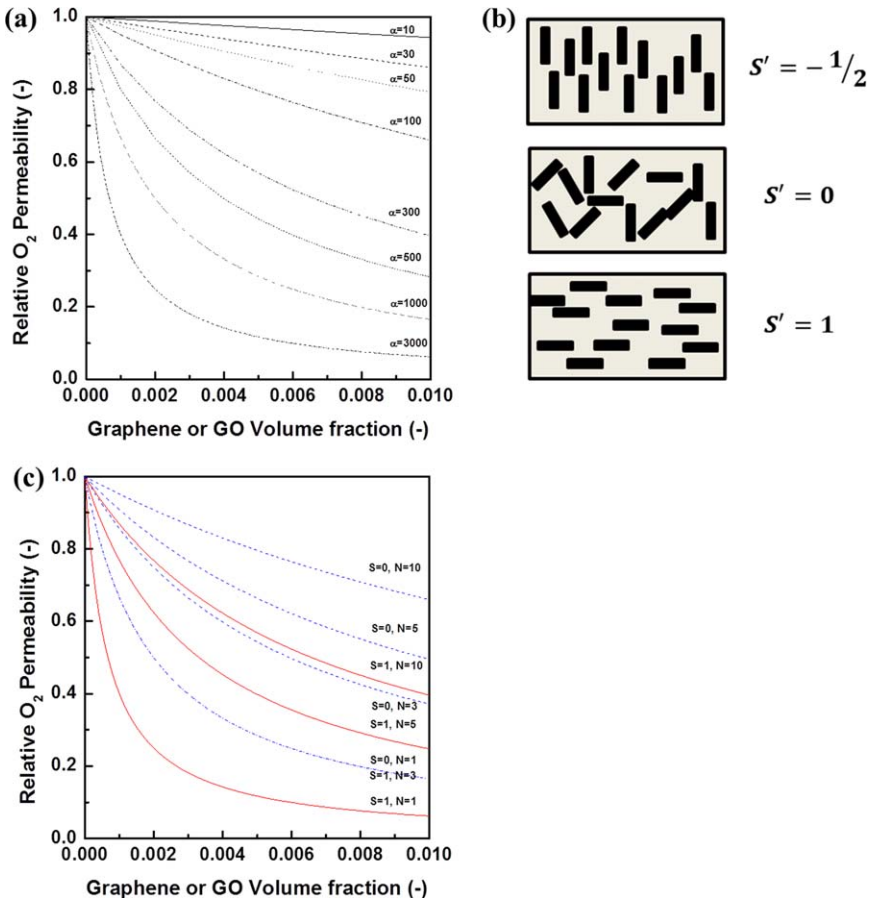

Figure 6. Gas transport in graphene/polymer nanocomposites: (a) effect of the graphene nanoplatelet size, (b) S' for the orientations of graphene nanoplatelets in the polymer matrix, and (c) effect of the orientation and the number of graphene nanoplatelet layers ($\alpha = 3000$). [Color figure can be viewed in the online issue, which is available at wileyonlinelibrary.com.]

dioxide,[201] sol–gel,[202] and covulcanization[203] methods are widely used to prepare graphene/polymer nanocomposites.[176]

Gas Transport in Graphene/Polymer Nanocomposites

Effect of the Graphene Nanoplatelet Size. The barrier properties of graphene/polymer nanocomposites can be enhanced by the insertion of inorganic fillers, especially layered-structure fillers, to extend the gas-diffusion path.[204] Some researchers have proposed various simple models for determining the gas-transport behavior through polymer nanocomposites filled with inorganic nanoplatets.[178,205–208] One of the advantages of graphene over other inorganic fillers is its high α, which extends the tortuosity of the path of diffusing gas molecules in the nanocomposites. A simple model including regularly arranged inorganic plates in the polymer matrix was proposed by Nielsen,[206] as presented in Figure 4(e). The impermeable inorganic platelets in the permeable polymer matrix can create tortuous, long pathways for diffusing gas molecules.[177,209,210] According to the solution–diffusion model, the gas permeability in polymer membranes can be expressed as a product of the diffusivity and solubility as follows:

$$P = DS \tag{3}$$

where P is the gas permeability of the polymeric membrane, D is the diffusivity of the gas molecules through the membranes, and S is the solubility of the gas molecules in the membranes. The solubility of nanocomposites can be expressed as a function of the volume fraction of the filler as follows:

$$S = S_0(1-\phi) \tag{4}$$

where S_0 is the solubility of the pure polymer matrix and ϕ is the volume fraction of the inorganic fillers.[211] The diffusivity of nanocomposites can be expressed with tortuosity as follows:

$$D = \frac{D_0}{\tau} \tag{5}$$

where D_0 is the diffusivity of the pure polymer matrix.[176] Tortuosity (τ) is defined as:

$$\tau \equiv \frac{l}{l'} \tag{6}$$

where l' is the distance between tortuous pathways through the membrane and l is the membrane thickness, that is, the shortest pathways for gas molecules.[211] From eqs. (3), (4), and (5):

$$\frac{P}{P_0} = \frac{1-\phi}{\tau} \tag{7}$$

where P_0 is the gas permeability of pure polymer matrix. If N is defined as the average number of inorganic platelets

$$l' = l + N \cdot \frac{L}{2} \tag{8}$$

Because $N = l(\phi/W)$, τ can be rewritten as follows:

$$\tau = 1 + \frac{L}{2W} \cdot \phi \tag{9}$$

From eqs. (7) and (9):

$$\frac{P}{P_0} = \frac{1-\phi}{1+\frac{\alpha}{2}\phi} \tag{10}$$

where $\alpha = L/W$ is the aspect ratio of the platelets. This equation can be used only when $\varphi \leq 0.1$ because the inorganic fillers tend to aggregate with increasing ϕ.[211] The predicted gas permeation models for different α are presented in Figure 6(a).

Effect of the Orientation and Number of Graphene Nanoplatelet Layers. The stacking orientation of graphene layers in a polymer matrix and self-aggregation of graphene nanoplatelets are important factors influencing the gas permeability of nanocomposites.[211,212] Nielsen's equation[206] is expressed as follows:

$$\frac{P}{P_0} = \frac{1-\phi}{1+\frac{\alpha}{2}\cdot\frac{2}{3}\left(S'+\frac{1}{2}\right)\phi} \tag{11}$$

where S' is the order parameter representing orientations of inorganic platelets, as presented in Figure 6(b). In the case of a high filler loading, eq. (10) can be rewritten with consideration of the degree of stacking with the parameter N.[213,214] Therefore, the equation can be expressed as follows:

$$\frac{P}{P_0} = \frac{1-\phi}{1+\frac{\alpha}{2N}\phi} \tag{12}$$

From eqs. (11) and (12)

$$\frac{P}{P_0} = \frac{1-\phi}{1+\frac{\alpha}{3N}\left(S'+\frac{1}{2}\right)\phi} \tag{13}$$

As shown in Figure 6(b), polymer/inorganic nanocomposites are supposed to have three types of orientations corresponding to three S's. As mentioned earlier, with the supposition that gas transport occurs between graphene nanoplatelets and the polymer matrix (rather than the interlayer between graphene nanoplatelets), a main factor in improving the gas-barrier properties in polymer nanocomposites will be the tortuosity. For $S' = 1$, that is, in the case of a horizontally stacked structure, graphene nanoplatelets can maximize the tortuosity; therefore, this structure will significantly decrease the gas permeation rate through the resulting nanocomposites.[211] However, when the degree of nanoplatelet stacking (N) is increased, the overall tortuosity of the polymer matrix will much lower; therefore, the barrier properties of the polymer nanocomposite will be relatively low. The predicted gas permeance results for different N and S' values when $\alpha = 3000$ are shown in Figure 6(c). As graphene nanoplatelets tend to aggregate, that is, as the value of N is increased, the gas-barrier properties significantly decline. This is because the aggregated graphene or GO nanoplatelets increase the probability that gas molecules flow through the relatively highly permeable polymer matrix rather than graphene or GO as compared with a well-dispersed and exfoliated graphene/polymer nanocomposite with same volume fraction of graphene or GO. These phenomena are related to the compatibility in the interfaces between the polymer and GO. The polar groups of GO basically provide compatibility with the polymer. Well-dispersed GO shows high compatibility because of biplanar polar groups; therefore, this also indicates an improved gas-barrier performance with long diffusional pathways. Aggregated GO platelets, however, show reduced compatibility with the polymer matrix, and thus, the polymer exhibits a low gas-barrier performance with decreased diffusional pathways. In the case of a fully exfoliated ($N = 1$) and horizontally stacked ($S' = 1$) graphene in a polymer matrix, an only 1 vol % addition of graphene nanoplatelets can reduce the gas permeability by a factor of 10 relative to that of the pure polymer matrix. However, in the case of 10-layer-stacked ($N = 10$) and randomly oriented ($S' = 0$) graphene in a polymer matrix, 1 vol % graphene nanoplatelets show only a 30% reduction in the original gas permeability. Accordingly, the orientation and the degree of exfoliation are very important for achieving improved gas-barrier properties in graphene/polymer nanocomposites.

Effect of the Thermal Shrinkage of Graphene. In general, the incorporation of a well-dispersed inorganic filler with a high intrinsic thermal stability and α can enhance the thermal stability of nanocomposites.[215] For this purpose, graphene is also a promising material suitable for thermally stable polymer nanocomposites. In general, graphene has a lower interfacial thermal resistance than CNTs because the sheetlike shape of graphene contacting the polymer matrix is more conductive compared to tube-shaped CNTs. Therefore, graphene is much more favorable for nanocomposites in the improvement of their thermal stability.[196,197,215] Moreover, the negative coefficient of thermal expansion (CTE)[216] of graphene can lead to a lower CTE for graphene/polymer nanocomposites.[197,204] At room temperature, graphene and GO have negative CTEs (-4.8×10^{-6} K^{-1} [217] and -50×10^{-6} K^{-1} [145], respectively) compared to the large, positive CTEs of typical polymers (10–500 $\times$ 10^{-6}/K). Therefore, such small, negative CTE values will lead to relatively low dimensional deformation of the nanocomposites when graphene is properly incorporated into the matrix.[192] However, the different CTEs between graphene and the polymer matrix may result in local fine defects during thermal treatment. Although the overall CTEs of nanocomposites may be reduced through the incorporation of graphene into a polymer matrix, such local fine defects on the interfaces between graphene and the polymer matrix might decrease the gas-barrier properties of the nanocomposites.

Graphene/Polymer Nanocomposites for Gas-Barrier Applications

The oxygen permeabilities of some graphene/polymer nanocomposites in the literature are presented as a function of graphene content in Figure 7(a).[218–224] Despite many efforts to improve the gas-barrier properties of graphene/polymer nanocomposites, the oxygen permeability, which is an important parameter for

Applied Polymer SCIENCE

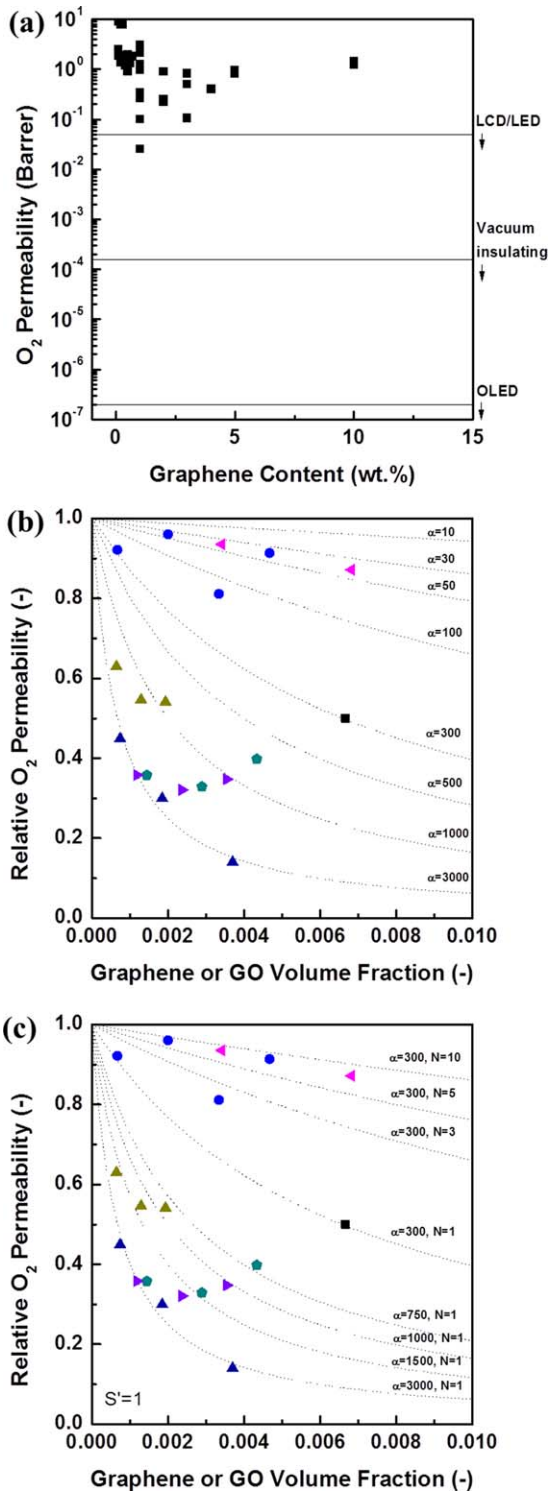

Figure 7. Applications of graphene/polymer nanocomposites as gas barriers: (a) O_2 permeability of graphene/polymer nanocomposites for graphene content, (b) effect of the graphene nanoplatelet sizes on the relative permeability, and (c) effect of the orientation and the number of graphene nanoplatelet layers on the relative permeability. [Color figure can be viewed in the online issue, which is available at wileyonlinelibrary.com.]

food packaging and encapsulated polymer films in electronic devices, is still too high to be used for vacuum-insulating and OLED barrier applications. Some examples of the relative oxygen permeability as a function of graphene or GO volume fraction[160,161,193–198] are presented in Figure 7(b,c). In Figure 7(b), the dotted lines represent the effect of α of graphene nanoplatelets with the assumption that graphene or GO is totally dispersed, fully exfoliated, in a single layer, and also horizontally stacked perpendicular to the gas-diffusion direction. For example, for the GO/polyimide (PI) nanocomposites (upper left, blue circles), when α is supposed to be 300, the experimental value is higher than the calculated value. In contrast, for GO/polyethylene glycol diacrylate (PEGDA) hydrogel nanocomposites (middle left, olive triangle), at the same α, the experimental value is lower than the theoretical value. These results might have been due to the different preparation methods, which resulted in different degrees of dispersion in the polymers. The GO/PI nanocomposites were prepared by solution mixing with a polar organic solvent, dimethylformamide, whereas the GO/PEGDA hydrogel nanocomposites were synthesized by *in situ* polymerization in water as a solvent. Therefore, the dispersion of GO in a polymer matrix in a GO/PEGDA hydrogel (because of hydrophilicity) was better than that of the GO/PI nanocomposites. In addition, the GO solubility in water was higher than that in dimethylformamide.[225] Moreover, crosslinking between GO and a hydrophilic PEGDA matrix by a crosslinking agent formed covalent bonding, which was stronger than van der Waals forces between GO in PI. However, when the proper surfactant was introduced into a polymer matrix for better dispersion of GO, the experimental gas permeability became close to the theoretical value. For example, GO/PI nanocomposites with Triton X-100 as a surfactant showed an oxygen permeability similar to the theoretical value. A surfactant prevents the aggregation of GO platelets in a polymer matrix and maintains the

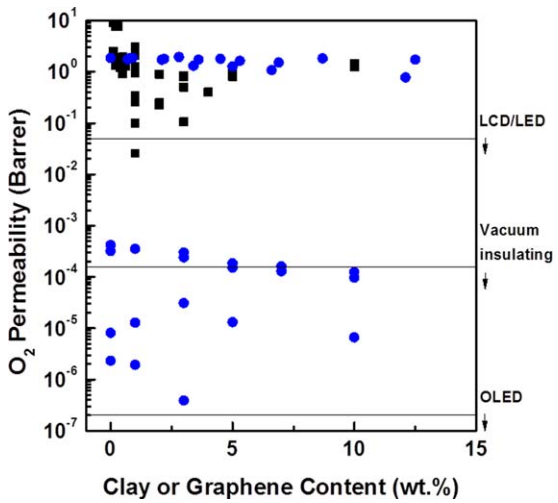

Figure 8. Schematic O_2 permeability of clay or graphene/polymer nanocomposites. (Black rectangles represent graphene/polymer nanocomposites and blue circles represent clay/polymer nanocomposites. [Color figure can be viewed in the online issue, which is available at wileyonlinelibrary.com.]

original high α, and, as a result, the oxygen permeability reaches the theoretical value.

Similar to the GO/PI nanocomposites mentioned previously, the expanded graphite/cellulose (CA) nanocomposites (upper middle, pink left triangle)[219] prepared by solution mixing ($\alpha = 1500$) showed a higher gas permeability than the theoretical ones because of the severe aggregation of expanded graphite in a solution-mixing state. On the other hand, similar to the GO/PEGDA nanocomposites mentioned previously, the GO/polyaniline (PANI) nanocomposites (lower left, blue triangle)[224] prepared by *in situ* polymerization ($\alpha = 3000$) exhibited lower than theoretical gas permeability because of the relatively better dispersion of *in situ* polymerization versus that of solution mixing.

Meanwhile, there are no significant differences between graphene and GO when the concentration is sufficiently high. In the case of expanded graphite/poly(lactic acid) (PLA) nanocomposites (lower left, violet right triangle, $\alpha = 3000$ and prepared by solution mixing) and GO/PLA nanocomposites (lower left, green pentagon, $\alpha = 3000$ and fabricated by solution mixing),[218] the ratio of gas permeability reduction was very similar, regardless of whether GO or expanded graphite was used. In both cases, when the concentrations of expanded graphene or GO were increased, both fillers tended to self-aggregate; this led to a slight reduction in the gas permeability because of the reduced tortuosity in the polymer matrix.

There have been many attempts to use graphene-based materials as inorganic nanofillers to enhance the physical properties of polymer nanocomposites and also to provide enhanced gas-barrier properties because of their high α,[226] good dispersion in common solvents,[114] and intrinsic high thermal stability, electrical conductivity, and mechanical strength.[227,228] Graphene/polymer nanocomposites also exhibit significantly improved electrical conductivity, mechanical strength, and thermal stability.[229] With regard to the gas-barrier properties of graphene/polymer nanocomposites, however, as shown in Figure 8, common graphene/polymer nanocomposites (black rectangles) still show relatively lower oxygen barrier properties than clay/polymer nanocomposites (blue circles), which are widely used for typical inorganic fillers,[218–224,230] despite numerous studies on the use of graphene for barrier applications in polymer nanocomposites.[206] However, there is great potential for improving the gas-barrier properties of graphene/polymer nanocomposites if we can control the size of the graphene or GO (or rGO) nanoplatelets,[206] the degree of dispersion, the graphene orientation, the number of graphene layers,[204] and the CTE between graphene and the polymer matrix.[231] The nanoplatelet size, which determines the high α, is a key factor in improving the gas-barrier properties as compared to typical inorganic nanofillers. The relatively high α of graphene-based 2D materials can certainly allow much longer pathways compared to other nanofillers if they can be fully exfoliated and well-dispersed in polymer nanocomposites.[204] The stacking structures of layered graphene also represents a crucial factor affecting the gas-barrier properties.[206] Horizontally, highly interlocked, stacked graphene structures with fully exfoliated graphene sheets may maximize the gas-barrier properties in graphene/polymer nanocomposites.[204] The difference in the CTE between graphene and the polymer matrix will be a relatively minor element compared to the two factors mentioned previously. However, local defects in the interphases between aggregated graphene particles and the polymer matrix due to a large difference in CTE values could be formed in a thermal drying process and may reduce the gas-barrier performance of the nanocomposites.[204] In addition, transparency is a minor issue for the intrinsic purpose of the barrier materials but is crucial in the food packaging industry.[1,2] The graphene monolayer itself is highly transparent; however, graphene derivatives, such as GO and rGO, lose their transparency and are colored because of aggregation. Furthermore, in the case of polymer/graphene nanocomposites, even a small portion of graphene derivatives makes them black. Thus, efforts to improve the transparency of graphene-incorporated gas-barrier materials for packaging purposes should be conducted.

These factors limit the gas-barrier performance of graphene/polymer nanocomposites; therefore, advanced techniques for the complete exfoliation of graphene sheets, homogeneous dispersion, and methods to prevent aggregation of graphene platelets in a polymer matrix and enhance their structural stability at high temperature should be developed to achieve a breakthrough in the gas-barrier properties of graphene/polymer nanocomposites. If these issues could be addressed properly, we could easily and inexpensively produce graphene/polymer nanocomposites for high gas-barrier polymeric films with high processability.

CONCLUSIONS

Defect-free, single crystal graphene is the perfect barrier material. Furthermore, graphene has a high mechanical strength, thermal stability, and electrical conductivity with a high transparency. Thus, graphene has been highlighted as a strong candidate for gas-barrier materials. On the basis of these advantages, many applications have been investigated, including pore-tuned graphene molecular filters and graphene layers to prevent metal corrosion. However, the manufacture of graphene by physical methods in industrial fields is fraught with problems, including defective graphene layers and difficulties in scale-up.

An alternative to mitigate the weaknesses of graphene is to use GO, that is, chemically functionalized graphene sheets with oxygen groups. GO is easily dispersed in common solvents; thus, it is more suitable for mass production and common use than graphene. Although GO is susceptible to humidity and has defects on the basal plane, the multistacked GO layers provide a long diffusion path, which results in low gas permeability. With GO considered as a precursor of graphene, rGO can also be a promising candidate for gas-barrier materials. However, the deformation of GO sheets during the reduction process still limits the formation of rGO films for gas-barrier applications.

For graphene/polymer nanocomposites, the platelet size, stacking orientation, and degree of graphene exfoliation in the polymer matrix are governing factors in determining the gas transport. In addition, the high mechanical strength, thermal

stability, and electrical conductivity with high transparency of graphene allow excellent applications with graphene/polymer nanocomposites. However, local defects of the nanocomposites during preparation, the aggregation of graphene derivatives at high graphene contents, and poor dispersability in organic solvents limit the mass production of graphene/polymer nanocomposites.

The theoretically perfect barrier properties of graphene have been the basis for many studies of the use of graphene and GO as perfect gas-barrier materials with the improvement of the synthesis process and multistacking techniques. Also, techniques to improve graphene's degree of exfoliation, dispersion, and orientation in a polymer matrix while also maintaining the other advantages of both graphene and the polymer for graphene/polymer nanocomposites have been studied extensively. If we can control those critical factors in graphene utilization, we can achieve a renaissance in the use of inexpensive carbon materials to meet the most demanding gas-barrier challenges faced today.

ACKNOWLEDGMENTS

This work was supported by grants from the Korea CCS R&D Center, funded by the Ministry of Education, Science, and Technology of the Korean government.

REFERENCES

1. Azeredo, H. M. C. D. *Food Res. Int.* **2009**, *42*, 1240.
2. Arora, A.; Padua, G. W. *J. Food Sci.* **2010**, *75*, R43.
3. Park, J. S.; Chae, H.; Chung, H. K.; Lee, S. I. *Semicond. Sci. Technol.* **2011**, *26*, 034001.
4. Hu, A.; Guo, J.; Alarifi, H.; Patane, G.; Zhou, Y.; Compagnini, G.; Xu, C. *Appl. Phys. Lett.* **2010**, *97*, 153113.
5. Lange, J.; Wyser, Y. *Packaging Technol. Sci.* **2003**, *16*, 149.
6. Spee, D.; Bakker, R.; van der Werf, C.; van Steenbergen, M.; Rath, J.; Schropp, R. *Thin Solid Films* **2011**, *519*, 4479.
7. Yang, Y. H.; Haile, M.; Park, Y. T.; Malek, F. A.; Grunlan, J. C. *Macromolecules* **2011**, *44*, 1450.
8. Holden, P.; Orchard, G.; Ward, I. *J. Polym. Sci. Part B: Polym. Phys.* **2003**, *23*, 709.
9. Nagai, I.; Tanaka, S.; Asakura, M. EP19960113333 (**1996**).
10. Hu, Y.; Prattipati, V.; Mehta, S.; Schiraldi, D.; Hiltner, A.; Baer, E. *Polymer* **2005**, *46*, 2685.
11. Massey, L. K. Permeability Properties of Plastics and Elastomers: A Guide to Packaging and Barrier Materials; Plastics Design Library/William Andrew Publishing: **2003**.
12. Jung, K. H.; Bae, J. Y.; Park, S. J.; Yoo, S.; Bae, B. S. *J. Mater. Chem.* **2010**, *21*, 1977.
13. Dameron, A. A.; Davidson, S. D.; Burton, B. B.; Carcia, P. F.; McLean, R. S.; George, S. M. *J. Phys. Chem. C* **2008**, *112*, 4573.
14. Hirvikorpi, T.; Vähä-Nissi, M.; Mustonen, T.; Iiskola, E.; Karppinen, M. *Thin Solid Films* **2010**, *518*, 2654.
15. Jia, Z.; Tucker, M. B.; Li, T. *Compos. Sci. Technol.* **2011**, *71*, 365.
16. Lu, N. S.; Wang, X.; Suo, Z. G.; Vlassak, J. *J. Mater. Res.* **2009**, *24*, 379.
17. Bunch, J. S.; Verbridge, S. S.; Alden, J. S.; Van Der Zande, A. M.; Parpia, J. M.; Craighead, H. G.; McEuen, P. L. *Nano Lett.* **2008**, *8*, 2458.
18. Leenaerts, O.; Partoens, B.; Peeters, F. *Appl. Phys. Lett.* **2008**, *93*, 193107.
19. Lee, C.; Wei, X.; Kysar, J. W.; Hone, J. *Science* **2008**, *321*, 385.
20. Nair, R.; Blake, P.; Grigorenko, A.; Novoselov, K.; Booth, T.; Stauber, T.; Peres, N.; Geim, A. *Science* **2008**, *320*, 1308.
21. Huang, P. Y.; Ruiz-Vargas, C. S.; van der Zande, A. M.; Whitney, W. S.; Levendorf, M. P.; Kevek, J. W.; Garg, S.; Alden, J. S.; Hustedt, C. J.; Zhu, Y. *Nature* **2011**, *469*, 389.
22. Batzill, M. *Surf. Sci. Rep.* **2012**, *67*, 83.
23. Lee, Y.; Bae, S.; Jang, H.; Jang, S.; Zhu, S. E.; Sim, S. H.; Song, Y. I.; Hong, B. H.; Ahn, J. H. *Nano Lett.* **2010**, *10*, 490.
24. Dreyer, D. R.; Park, S.; Bielawski, C. W.; Ruoff, R. S. *Chem. Soc. Rev.* **2010**, *39*, 228.
25. Robinson, J. T.; Zalalutdinov, M.; Baldwin, J. W.; Snow, E. S.; Wei, Z.; Sheehan, P.; Houston, B. H. *Nano Lett.* **2008**, *8*, 3441.
26. Zhao, J.; Pei, S.; Ren, W.; Gao, L.; Cheng, H. M. *Am. Chem. Soc. Nano* **2010**, *4*, 5245.
27. Sun, P.; Zhu, M.; Wang, K.; Zhong, M.; Wei, J.; Wu, D.; Xu, Z.; Zhu, H. *Am. Chem. Soc. Nano* **2013**, *7*, 428.
28. Yu, L.; Lim, Y.-S.; Han, J. H.; Kim, K.; Kim, J. Y.; Choi, S.-Y.; Shin, K. *Synth. Met.* **2012**, *162*, 710.
29. Usuki, A.; Kawasumi, M.; Kojima, Y.; Okada, A.; Kurauchi, T.; Kamigaito, O. *J. Mater. Res.* **1993**, *8*, 1174.
30. Priolo, M. A.; Gamboa, D.; Holder, K. M.; Grunlan, J. C. *Nano Lett.* **2010**, *10*, 4970.
31. LeBaron, P. C.; Wang, Z.; Pinnavaia, T. *J. Appl. Clay Sci.* **1999**, *15*, 11.
32. Jacquelot, E.; Espuche, E.; Gérard, J. F.; Duchet, J.; Mazabraud, P. *J. Polym. Sci. Part B: Polym. Phys.* **2005**, *44*, 431.
33. Nazarenko, S.; Meneghetti, P.; Julmon, P.; Olson, B.; Qutubuddin, S. *J. Polym. Sci. Part B: Polym. Phys.* **2007**, *45*, 1733.
34. Herrera-Alonso, J. M.; Marand, E.; Little, J. C.; Cox, S. S. *J. Membr. Sci.* **2009**, *337*, 208.
35. Liang, Y.; Cao, W.; Li, Z.; Wang, Y.; Wu, Y.; Zhang, L. *Polym. Test.* **2008**, *27*, 270.
36. Minelli, M.; De Angelis, M. G.; Doghieri, F.; Marini, M.; Toselli, M.; Pilati, F. *Eur. Polym. J.* **2008**, *44*, 2581.
37. Pannirselvam, M. *eXPRESS Polym. Lett.* **2008**, *2*, 429.
38. Liu, A.; Walther, A.; Ikkala, O.; Belova, L.; Berglund, L. A. *Biomacromolecules* **2011**, *12*, 633.
39. Usuki, A.; Hasegawa, N.; Kato, M. *Inorg. Polym. Nanocompos. Membr.* **2005**, *179*, 135.

40. Nazarenko, S.; Meneghetti, P.; Julmon, P.; Olson, B. G.; Qutubuddin, S. *J. Polym. Sci. Part B: Polym. Phys.* **2007**, *45*, 1733.
41. Heller, H.; Keren, R. *Clays Clay Mineral* **2001**, *49*, 286.
42. Olad, A. *Polymer/Clay Nanocomposites; InTech*: **2011**.
43. Suk, J. W.; Piner, R. D.; An, J.; Ruoff, R. S. *Am. Chem. Soc. Nano* **2010**, *4*, 6557.
44. Novoselov, K.; Geim, A.; Morozov, S.; Jiang, D.; Zhang, Y.; Dubonos, S.; Grigorieva, I.; Firsov, A. *Science* **2004**, *306*, 666.
45. Jiang, J. W.; Wang, J. S.; Li, B. *Phys. Rev. B* **2009**, *80*, 113405.
46. Balandin, A. A.; Ghosh, S.; Bao, W.; Calizo, I.; Teweldebrhan, D.; Miao, F.; Lau, C. N. *Nano Lett.* **2008**, *8*, 902.
47. McAllister, M. J.; Li, J. L.; Adamson, D. H.; Schniepp, H. C.; Abdala, A. A.; Liu, J.; Herrera-Alonso, M.; Milius, D. L.; Car, R.; Prud'homme, R. K. *Chem. Mater.* **2007**, *19*, 4396.
48. Bolotin, K. I.; Sikes, K.; Jiang, Z.; Klima, M.; Fudenberg, G.; Hone, J.; Kim, P.; Stormer, H. *Solid State Commun.* **2008**, *146*, 351.
49. Wu, Z. S.; Ren, W.; Gao, L.; Liu, B.; Jiang, C.; Cheng, H. M. *Carbon* **2009**, *47*, 493.
50. Maiti, A.; Svizhenko, A.; Anantram, M. *Phys. Rev. Lett.* **2002**, *88*, 126805.
51. Reina, A.; Jia, X.; Ho, J.; Nezich, D.; Son, H.; Bulovic, V.; Dresselhaus, M. S.; Kong, J. *Nano Lett.* **2008**, *9*, 30.
52. Kim, K. S.; Zhao, Y.; Jang, H.; Lee, S. Y.; Kim, J. M.; Ahn, J. H.; Kim, P.; Choi, J. Y.; Hong, B. H. *Nature* **2009**, *457*, 706.
53. Berger, C.; Song, Z.; Li, X.; Wu, X.; Brown, N.; Naud, C.; Mayou, D.; Li, T.; Hass, J.; Marchenkov, A. N. *Science* **2006**, *312*, 1191.
54. Xu, Z.; Gao, C. *Macromolecules* **2010**, *43*, 6716.
55. Kosynkin, D. V.; Higginbotham, A. L.; Sinitskii, A.; Lomeda, J. R.; Dimiev, A.; Price, B. K.; Tour, J. M. *Nature* **2009**, *458*, 872.
56. Jiao, L.; Zhang, L.; Wang, X.; Diankov, G.; Dai, H. *Nature* **2009**, *458*, 877.
57. Zhu, Y. W.; Murali, S.; Cai, W. W.; Li, X. S.; Suk, J. W.; Potts, J. R.; Ruoff, R. S. *Adv. Mater.* **2010**, *22*, 3906.
58. Duong, D. L.; Han, G. H.; Lee, S. M.; Gunes, F.; Kim, E. S.; Kim, S. T.; Kim, H.; Ta, Q. H.; So, K. P.; Yoon, S. J.; Chae, S. J.; Jo, Y. W.; Park, M. H.; Chae, S. H.; Lim, S. C.; Choi, J. Y.; Lee, Y. H. *Nature* **2012**, *490*, 235.
59. Koenig, S. P.; Wang, L.; Pellegrino, J.; Bunch, J. S. *Nat. Nano* **2012**, *7*, 728.
60. O'Hern, S. C.; Stewart, C. A.; Boutilier, H., M. S.; Idrobo, J.-C.; Bhaviripudi, S.; Das, S. K.; Kong, J.; Laoui, T.; Atieh, M.; Karnik, R. *Am. Chem. Soc. Nano* **2012**, *6*, 10130.
61. Qin, X.; Meng, Q.; Feng, Y.; Gao, Y. *Surf. Sci.* **2012**, *607*, 153.
62. Blankenburg, S.; Bieri, M.; Fasel, R.; Müllen, K.; Pignedoli, C. A.; Passerone, D. *Small* **2010**, *6*, 2266.
63. Schrier, J. *J. Phys. Chem. Lett.* **2010**, *1*, 2284.
64. Bae, S.; Kim, H.; Lee, Y.; Xu, X.; Park, J. S.; Zheng, Y.; Balakrishnan, J.; Lei, T.; Kim, H. R.; Song, Y. I. *Nat. Nanotechnol.* **2010**, *5*, 574.
65. Koenig, S. P.; Wang, L. D.; Pellegrino, J.; Bunch, J. S. *Nat. Nanotechnol.* **2012**, *7*, 728.
66. Novoselov, K.; Jiang, D.; Schedin, F.; Booth, T.; Khotkevich, V.; Morozov, S.; Geim, A. Proc. Natl. Acad. Sci. USA **2005**, *102*, 10451.
67. Koenig, S. P.; Boddeti, N. G.; Dunn, M. L.; Bunch, J. S. *Nat. Nanotechnol.* **2011**, *6*, 543.
68. Shivaraman, S.; Barton, R. A.; Yu, X.; Alden, J.; Herman, L.; Chandrashekhar, M.; Park, J.; McEuen, P. L.; Parpia, J. M.; Craighead, H. G. *Nano Lett.* **2009**, *9*, 3100.
69. Alemán, B.; Regan, W.; Aloni, S.; Altoe, V.; Alem, N.; Girit, C.; Geng, B.; Maserati, L.; Crommie, M.; Wang, F. *Am. Chem. Soc. Nano* **2010**, *4*, 4762.
70. Lin, Y. C.; Jin, C.; Lee, J. C.; Jen, S. F.; Suenaga, K.; Chiu, P. W. *Am. Chem. Soc. Nano* **2011**, *5*, 2362.
71. Hauser, A. W.; Schwerdtfeger, P. *J. Phys. Chem. Lett.* **2012**, *3*, 209.
72. Hauser, A. W.; Schwerdtfeger, P. *Phys. Chem. Chem. Phys.* **2012**, *14*, 13292.
73. Drahushuk, L. W.; Strano, M. S. *Langmuir* **2012**, *28*, 16671.
74. Nilsson, L.; Andersen, M.; Balog, R.; Lægsgaard, E.; Hofmann, P.; Besenbacher, F.; Hammer, B.; Stensgaard, I.; Hornekaer, L. *Am. Chem. Soc. Nano* **2012**, *6*, 10258.
75. Chen, S. S.; Brown, L.; Levendorf, M.; Cai, W. W.; Ju, S. Y.; Edgeworth, J.; Li, X. S.; Magnuson, C. W.; Velamakanni, A.; Piner, R. D.; Kang, J. Y.; Park, J.; Ruoff, R. S. *Am. Chem. Soc. Nano* **2011**, *5*, 1321.
76. Kang, D.; Kwon, J. Y.; Cho, H.; Sim, J. H.; Hwang, H. S.; Kim, C. S.; Kim, Y. J.; Ruoff, R. S.; Shin, H. S. *Am. Chem. Soc. Nano* **2012**, *6*, 7763.
77. Kirkland, N.; Schiller, T.; Medhekar, N.; Birbilis, N. *Corros. Sci.* **2011**, *56*, 1.
78. Prasai, D.; Tuberquia, J. C.; Harl, R. R.; Jennings, G. K.; Bolotin, K. I. *Am. Chem. Soc. Nano* **2012**, *6*, 1102.
79. Singh Raman, R.; Chakraborty Banerjee, P.; Lobo, D. E.; Gullapalli, H.; Sumandasa, M.; Kumar, A.; Choudhary, L.; Tkacz, R.; Ajayan, P. M.; Majumder, M. *Carbon* **2012**, *50*, 4040.
80. Jiang, D.; Cooper, V. R.; Dai, S. *Nano Lett.* **2009**, *9*, 4019.
81. Hauser, A. W.; Schwerdtfeger, P. *J. Phys. Chem. Lett.* **2012**, *3*, 209.
82. Sint, K.; Wang, B.; Král, P. *J. Am. Chem. Soc.* **2008**, *130*, 16448.
83. Cohen-Tanugi, D.; Grossman, J. C. *Nano Lett.* **2012**, *12*, 3602.
84. Hu, G.; Mao, M.; Ghosal, S. *Nanotechnology* **2012**, *23*, 395501.
85. Lee, J.; Aluru, N. *J. Membr. Sci.* **2012**, *428*, 546.
86. Fischbein, M. D.; Drndic, M. *Appl. Phys. Lett.* **2008**, *93*, 113103.
87. Chen, S.; Brown, L.; Levendorf, M.; Cai, W.; Ju, S. Y.; Edgeworth, J.; Li, X.; Magnuson, C.; Velamakanni, A.; Piner, R. R. *Am. Chem. Soc. Nano* **2010**, *5*, 1321.
88. Pushpavanam, M.; Raman, V.; Shenoi, B. *Surf. Technol.* **1981**, *12*, 351.

89. Segarra, M.; Miralles, L.; Diaz, J.; Xuriguera, H.; Chimenos, J.; Espiell, F.; Pinol, S. *Mater. Sci. Forum* **2003**, *426*, 3511.
90. Tallman, D. E.; Spinks, G.; Dominis, A.; Wallace, G. G. *J. Solid State Electrochem.* **2002**, *6*, 73.
91. Lusk, A. T.; Jennings, G. K. *Langmuir* **2001**, *17*, 7830.
92. Appa Rao, B.; Yakub Iqbal, M.; Sreedhar, B. *Corros. Sci.* **2009**, *51*, 1441.
93. Strohmeier, B. R. *Surf. Interface Anal.* **1990**, *15*, 51.
94. Liu, L.; Ryu, S.; Tomasik, M. R.; Stolyarova, E.; Jung, N.; Hybertsen, M. S.; Steigerwald, M. L.; Brus, L. E.; Flynn, G. W. *Nano Lett.* **2008**, *8*, 1965.
95. De Heer, W. A.; Berger, C.; Wu, X.; First, P. N.; Conrad, E. H.; Li, X.; Li, T.; Sprinkle, M.; Hass, J.; Sadowski, M. L. *Solid State Commun.* **2007**, *143*, 92.
96. Masuda, T.; Isobe, E.; Higashimura, T.; Takada, K. *J. Am. Chem. Soc.* **1983**, *105*, 7473.
97. Robeson, L. M. *J. Membr. Sci.* **2008**, *320*, 390.
98. Suda, H.; Haraya, K. *J. Phys. Chem. B* **1997**, *101*, 3988.
99. Reina, A.; Son, H.; Jiao, L.; Fan, B.; Dresselhaus, M. S.; Liu, Z. F.; Kong, J. *J. Phys. Chem. C* **2008**, *112*, 17741.
100. Li, X.; Zhu, Y.; Cai, W.; Borysiak, M.; Han, B.; Chen, D.; Piner, R. D.; Colombo, L.; Ruoff, R. S. *Nano Lett.* **2009**, *9*, 4359.
101. Jiao, L.; Fan, B.; Xian, X.; Wu, Z.; Zhang, J.; Liu, Z. *J. Am. Chem. Soc.* **2008**, *130*, 12612.
102. Sinitskii, A.; Tour, J. M. *Appl. Phys. Lett.* **2012**, *100*, 103106.
103. Cho, J.; Gao, L.; Tian, J. F.; Cao, H. L.; Wu, W.; Yu, Q. K.; Yitamben, E. N.; Fisher, B.; Guest, J. R.; Chen, Y. P.; Guisinger, N. P. *Am. Chem. Soc. Nano* **2011**, *5*, 3607.
104. Wang, Y. J.; Miao, C. Q.; Huang, B. C.; Zhu, J.; Liu, W.; Park, Y.; Xie, Y. H.; Woo, J. C. S. *IEEE Trans. Electron Devices* **2010**, *57*, 3472.
105. Brodie, B. C. *Phil. Trans. R. Soc. London* **1859**, *149*, 249.
106. Hummers, W. S.; Offeman, R. E. *J. Am. Chem. Soc.* **1958**, *80*, 1339.
107. Lerf, A.; He, H.; Forster, M.; Klinowski, J. *J. Phys. Chem. B* **1998**, *102*, 4477.
108. He, H.; Klinowski, J.; Forster, M.; Lerf, A. *Chem. Phys. Lett.* **1998**, *287*, 53.
109. Cai, W.; Piner, R. D.; Stadermann, F. J.; Park, S.; Shaibat, M. A.; Ishii, Y.; Yang, D.; Velamakanni, A.; An, S. J.; Stoller, M. *Science* **2008**, *321*, 1815.
110. Eda, G.; Chhowalla, M. *Adv. Mater.* **2010**, *22*, 2392.
111. Kim, F.; Cote, L. J.; Huang, J. *Adv. Mater.* **2010**, *22*, 1954.
112. Li, X.; Zhang, G.; Bai, X.; Sun, X.; Wang, X.; Wang, E.; Dai, H. *Nat. Nanotechnol.* **2008**, *3*, 538.
113. Kudin, K. N.; Ozbas, B.; Schniepp, H. C.; Prud'homme, R. K.; Aksay, I. A.; Car, R. *Nano Lett.* **2008**, *8*, 36.
114. Dreyer, D. R.; Park, S.; Bielawski, C. W.; Ruoff, R. S. *Chem. Soc. Rev.* **2010**, *39*, 228.
115. Gomez-Navarro, C.; Weitz, R. T.; Bittner, A. M.; Scolari, M.; Mews, A.; Burghard, M.; Kern, K. *Nano Lett.* **2007**, *7*, 3499.
116. Park, S.; Ruoff, R. S. *Nat. Nanotechnol.* **2009**, *4*, 217.
117. Compton, O. C.; Nguyen, S. B. T. *Small* **2010**, *6*, 711.
118. Stankovich, S.; Piner, R. D.; Chen, X.; Wu, N.; Nguyen, S. B. T.; Ruoff, R. S. *J. Mater. Chem.* **2006**, *16*, 155.
119. Sun, X.; Liu, Z.; Welsher, K.; Robinson, J. T.; Goodwin, A.; Zaric, S.; Dai, H. *Nano Res.* **2008**, *1*, 203.
120. Jung, I.; Vaupel, M.; Pelton, M.; Piner, R.; Dikin, D. A.; Stankovich, S.; An, J.; Ruoff, R. S. *J. Phys. Chem. C* **2008**, *112*, 8499.
121. Luo, Z.; Lu, Y.; Somers, L. A.; Johnson, A. T. C. *J. Am. Chem. Soc.* **2009**, *131*, 898.
122. Sakhaee-Pour, A. *Solid State Commun.* **2009**, *149*, 91.
123. Gao, X. F.; Jang, J.; Nagase, S. *J. Phys. Chem. C* **2010**, *114*, 832.
124. Moon, I. K.; Lee, J.; Ruoff, R. S.; Lee, H. *Nat. Commun.* **2010**, *1*, 73.
125. Williams, G.; Seger, B.; Kamat, P. V. *Am. Chem. Soc. Nano* **2008**, *2*, 1487.
126. Becerril, H. A.; Mao, J.; Liu, Z.; Stoltenberg, R. M.; Bao, Z.; Chen, Y. *Am. Chem. Soc. Nano* **2008**, *2*, 463.
127. Wang, X.; Zhi, L.; Müllen, K. *Nano Lett.* **2008**, *8*, 323.
128. Stankovich, S.; Dikin, D. A.; Piner, R. D.; Kohlhaas, K. A.; Kleinhammes, A.; Jia, Y.; Wu, Y.; Nguyen, S. B. T.; Ruoff, R. S. *Carbon* **2007**, *45*, 1558.
129. Li, X.; Wang, X.; Zhang, L.; Lee, S.; Dai, H. *Science* **2008**, *319*, 1229.
130. Gómez-Navarro, C.; Weitz, R. T.; Bittner, A. M.; Scolari, M.; Mews, A.; Burghard, M.; Kern, K. *Nano Lett.* **2007**, *7*, 3499.
131. Mohanty, N.; Nagaraja, A.; Armesto, J.; Berry, V. *Small* **2009**, *6*, 226.
132. Li, J.; Lin, H.; Yang, Z. *Carbon* **2011**, *49*, 3024.
133. Zhang, J.; Yang, H.; Shen, G.; Cheng, P.; Guo, S. *Chem. Commun.* **2010**, *46*, 1112.
134. Moon, I. K.; Lee, J.; Ruoff, R. S.; Lee, H. *Nat. Commun.* **2010**, *1*, 73.
135. Wang, G.; Yang, J.; Park, J.; Gou, X.; Wang, B.; Liu, H.; Yao, J. *J. Phys. Chem. C* **2008**, *112*, 8192.
136. Chen, Y.; Zhang, X.; Yu, P.; Ma, Y. *Chem. Commun.* **2009**, *30*, 4527.
137. Fan, X.; Peng, W.; Li, Y.; Li, X.; Wang, S.; Zhang, G.; Zhang, F. *Adv. Mater.* **2008**, *20*, 4490.
138. Zhou, Y.; Bao, Q.; Tang, L. A. L.; Zhong, Y.; Loh, K. P. *Chem. Mater.* **2009**, *21*, 2950.
139. Zhu, Y.; Murali, S.; Stoller, M. D.; Velamakanni, A.; Piner, R. D.; Ruoff, R. S. *Carbon* **2010**, *48*, 2118.
140. Chen, W.; Yan, L.; Bangal, P. R. *Carbon* **2010**, *48*, 1146.
141. Gao, W.; Alemany, L. B.; Ci, L.; Ajayan, P. M. *Nat. Chem.* **2009**, *1*, 403.
142. Kim, M. C.; Hwang, G. S.; Ruoff, R. S. *J. Chem. Phys.* **2009**, *131*, 064704.
143. Gao, X.; Jang, J.; Nagase, S. *J. Phys. Chem. C* **2009**, *114*, 832.

144. Schniepp, H. C.; Li, J. L.; McAllister, M. J.; Sai, H.; Herrera-Alonso, M.; Adamson, D. H.; Prud'homme, R. K.; Car, R.; Saville, D. A.; Aksay, I. A. *J. Phys. Chem. B* **2006**, *110*, 8535.

145. Dikin, D. A.; Stankovich, S.; Zimney, E. J.; Piner, R. D.; Dommett, G. H. B.; Evmenenko, G.; Nguyen, S. B. T.; Ruoff, R. S. *Nature* **2007**, *448*, 457.

146. Li, D.; Müller, M. B.; Gilje, S.; Kaner, R. B.; Wallace, G. G. *Nat. Nanotechnol.* **2008**, *3*, 101.

147. Cote, L. J.; Kim, F.; Huang, J. *J. Am. Chem. Soc.* **2008**, *131*, 1043.

148. Su, C. Y.; Xu, Y.; Zhang, W.; Zhao, J.; Tang, X.; Tsai, C. H.; Li, L. *J. Chem. Mater.* **2009**, *21*, 5674.

149. Gilje, S.; Han, S.; Wang, M.; Wang, K. L.; Kaner, R. B. *Nano Lett.* **2007**, *7*, 3394.

150. Pham, V. H.; Cuong, T. V.; Hur, S. H.; Shin, E. W.; Kim, J. S.; Chung, J. S.; Kim, E. *J. Carbon* **2010**, *48*, 1945.

151. Lee, V.; Whittaker, L.; Jaye, C.; Baroudi, K. M.; Fischer, D. A.; Banerjee, S. *Chem. Mater.* **2009**, *21*, 3905.

152. Putz, K. W.; Compton, O. C.; Segar, C.; An, Z.; Nguyen, S. B. T.; Brinson, L. C. *Am. Chem. Soc. Nano* **2011**, *5*, 6601.

153. Pang, S.; Tsao, H. N.; Feng, X.; Müllen, K. *Adv. Mater.* **2009**, *21*, 3488.

154. Yamaguchi, H.; Eda, G.; Mattevi, C.; Kim, H. K.; Chhowalla, M. Am. Chem. Soc. Nano **2010**, *4*, 524.

155. Tung, V. C.; Allen, M. J.; Yang, Y.; Kaner, R. B. *Nat. Nanotechnol.* **2008**, *4*, 25.

156. Chen, C.; Yang, Q. H.; Yang, Y.; Lv, W.; Wen, Y.; Hou, P. X.; Wang, M.; Cheng, H. M. *Adv. Mater.* **2009**, *21*, 3007.

157. Xu, Y.; Sheng, K.; Li, C.; Shi, G. *Am. Chem. Soc. Nano* **2010**, *4*, 4324.

158. Chen, F.; Liu, S.; Shen, J.; Wei, L.; Liu, A.; Chan-Park, M. B.; Chen, Y. *Langmuir* **2011**, *27*, 9174.

159. Cheng, W.; Campolongo, M. J.; Tan, S. J.; Luo, D. *Nano Today* **2009**, *4*, 482.

160. Bai, H.; Li, C.; Shi, G. *Adv. Mater.* **2011**, *23*, 1089.

161. Kotov, N. A.; Dékány, I.; Fendler, J. H. *Adv. Mater.* **1996**, *8*, 637.

162. Nielsen, L. E. *J. Macromol. Sci. Chem.* **1967**, *1*, 929.

163. Choudalakis, G.; Gotsis, A. *Eur. Polym. J.* **2009**, *45*, 967.

164. Xu, Y.; Bai, H.; Lu, G.; Li, C.; Shi, G. *J. Am. Chem. Soc.* **2008**, *130*, 5856.

165. Liu, F.; Song, S.; Xue, D.; Zhang, H. *Adv. Mater.* **2012**, *8*, 1089.

166. Paul, D. R. *Science* **2012**, *335*, 413.

167. Zhang, L.; Liang, J.; Huang, Y.; Ma, Y.; Wang, Y.; Chen, Y. *Carbon* **2009**, *47*, 3365.

168. Eda, G.; Chhowalla, M. *Nano Lett.* **2009**, *9*, 814.

169. Medhekar, N. V.; Ramasubramaniam, A.; Ruoff, R. S.; Shenoy, V. B. *Am. Chem. Soc. Nano* **2010**, *4*, 2300.

170. Park, S.; Lee, K. S.; Bozoklu, G.; Cai, W.; Nguyen, S. B. T.; Ruoff, R. S. *Am. Chem. Soc. Nano* **2008**, *2*, 572.

171. Qiu, L.; Zhang, X.; Yang, W.; Wang, Y.; Simon, G. P.; Li, D. *Chem. Commun.* **2011**, *47*, 5810.

172. Nair, R.; Wu, H.; Jayaram, P.; Grigorieva, I.; Geim, A. *Science* **2012**, *335*, 442.

173. Park, S.; Dikin, D. A.; Nguyen, S. B. T.; Ruoff, R. S. *J. Phys. Chem. C* **2009**, *113*, 15801.

174. Singh, S.; Yadav, B. C.; Tandon, P.; Singh, M.; Shukla, A.; Dzhardimalieva, G. I.; Pomogailo, S. I.; Golubeva, N. D.; Pomogailo, A. D. *Sens. Actuators B* **2012**, *166*, 281.

175. Kumar, A. P.; Depan, D.; Singh Tomer, N.; Singh, R. P. *Prog. Polym. Sci.* **2009**, *34*, 479.

176. Chen, B.; Evans, J. R. G.; Greenwell, H. C.; Boulet, P.; Coveney, P. V.; Bowden, A. A.; Whiting, A. *Chem. Soc. Rev.* **2008**, *37*, 568.

177. Sinha Ray, S.; Okamoto, M. *Prog. Polym. Sci.* **2003**, *28*, 1539.

178. Bharadwaj, R. K. *Macromolecules* **2001**, *34*, 9189.

179. Usuki, A.; Hasegawa, N.; Kato, M. *Inorg. Polym. Nanocompos. Membr.* **2005**, *179*, 135.

180. Lan, T.; Kaviratna, P. D.; Pinnavaia, T. *J. Chem. Mater.* **1994**, *6*, 573.

181. Gain, O.; Espuche, E.; Pollet, E.; Alexandre, M.; Dubois, P. *J. Polym. Sci. Part B: Polym. Phys.* **2005**, *43*, 205.

182. Rodríguez-Cruz, M. S.; Sánchez-Martín, M. J.; Andrades, M. S.; Sánchez-Camazano, M. *J. Hazard. Mater.* **2007**, *139*, 363.

183. Sun, Q.; Schork, F. J.; Deng, Y. *Compos. Sci. Technol.* **2007**, *67*, 1823.

184. Park, S. J.; Seo, D. I.; Lee, J. R. *J. Colloid Interface Sci.* **2002**, *251*, 160.

185. Gorrasi, G.; Tortora, M.; Vittoria, V.; Pollet, E.; Lepoittevin, B.; Alexandre, M.; Dubois, P. *Polymer* **2003**, *44*, 2271.

186. Sinha Ray, S.; Bousmina, M. *Macromol. Rapid Commun.* **2005**, *26*, 1639.

187. Vickery, J. L.; Patil, A. J.; Mann, S. *Adv. Mater.* **2009**, *21*, 2180.

188. Ramanathan, T.; Abdala, A. A.; Stankovich, S.; Dikin, D. A.; Herrera Alonso, M.; Piner, R. D.; Adamson, D. H.; Schniepp, H. C.; Chen, X.; Ruoff, R. S.; Nguyen, S. T.; Aksay, I. A.; Prud'homme, R. K.; Brinson, L. C. *Nat. Nano* **2008**, *3*, 327.

189. Geim, A. K.; Novoselov, K. S. *Nat. Mater.* **2007**, *6*, 183.

190. Stankovich, S.; Dikin, D. A.; Dommett, G. H. B.; Kohlhaas, K. M.; Zimney, E. J.; Stach, E. A.; Piner, R. D.; Nguyen, S. T.; Ruoff, R. S. *Nature* **2006**, *442*, 282.

191. Rafiee, M. A.; Rafiee, J.; Srivastava, I.; Wang, Z.; Song, H.; Yu, Z.-Z.; Koratkar, N. *Small* **2010**, *6*, 179.

192. Kim, H.; Abdala, A. A.; Macosko, C. W. *Macromolecules* **2010**, *43*, 6515.

193. Nguyen, Q. T.; Baird, D. G. *Adv. Polym. Technol.* **2006**, *25*, 270.

194. Sengupta, R.; Bhattacharya, M.; Bandyopadhyay, S.; Bhowmick, A. K. *Prog. Polym. Sci.* **2011**, *36*, 638.

195. Verdejo, R.; Bernal, M. M.; Romasanta, L. J.; Lopez-Manchado, M. A. *J. Mater. Chem.* **2011**, *21*, 3301.

196. Potts, J. R.; Dreyer, D. R.; Bielawski, C. W.; Ruoff, R. S. *Polymer* **2011**, *52*, 5.

197. Du, J.; Cheng, H. M. *Macromol. Chem. Phys.* **2012**, *213*, 1060.

198. Hussain, F.; Hojjati, M.; Okamoto, M.; Gorga, R. E. *J. Compos. Mater.* **2006**, *40*, 1511.

199. Khaorapapong, N.; Kuroda, K.; Hashizume, H.; Ogawa, M. *Appl. Clay Sci.* **2001**, *19*, 69.

200. Xu, M.; Choi, Y. S.; Kim, Y. K.; Wang, K. H.; Chung, I. *J. Polymer* **2003**, *44*, 6387.

201. Zhao, Q.; Samulski, E. T. *Polymer* **2006**, *47*, 663.

202. Séquaris, J. M.; Baßmann, F.; Hild, A.; Narres, H. D.; Schwuger, M. *J. Colloids Surf. A* **1999**, *159*, 503.

203. Usuki, A.; Tukigase, A.; Kato, M. *Polymer* **2002**, *43*, 2185.

204. Paul, D. R.; Robeson, L. M. *Polymer* **2008**, *49*, 3187.

205. Fredrickson, G. H.; Bicerano, J. *J. Chem. Phys.* **1999**, *110*, 2181.

206. Nielsen, L. E. *J. Macromol. Sci. Chem.* **1967**, *1*, 929.

207. Takahashi, S.; Goldberg, H. A.; Feeney, C. A.; Karim, D. P.; Farrell, M.; O'Leary, K.; Paul, D. R. *Polymer* **2006**, *47*, 3083.

208. Lape, N. K.; Nuxoll, E. E.; Cussler, E. L. *J. Membr. Sci.* **2004**, *236*, 29.

209. Meille, S. V.; Bruckner, S.; Porzio, W. *Macromolecules* **1990**, *23*, 4114.

210. Gorrasi, G.; Tammaro, L.; Tortora, M.; Vittoria, V.; Kaempfer, D.; Reichert, P.; Mülhaupt, R. *J. Polym. Sci. Part B: Polym. Phys.* **2003**, *41*, 1798.

211. Choudalakis, G.; Gotsis, A. D. *Eur. Polym. J.* **2009**, *45*, 967.

212. Sun, L.; Boo, W. J.; Clearfield, A.; Sue, H. J.; Pham, H. Q. *J. Membr. Sci.* **2008**, *318*, 129.

213. Kim, H.; Macosko, C. W. *Polymer* **2009**, *50*, 3797.

214. Nazarenko, S.; Meneghetti, P.; Julmon, P.; Olson, B. G.; Qutubuddin, S. *J. Polym. Sci. Part B: Polym. Phys.* **2007**, *45*, 1733.

215. Cai, D.; Song, M. *J. Mater. Chem.* **2010**, *20*, 7906.

216. Fasolino, A.; Los, J. H.; Katsnelson, M. I. *Nat. Mater.* **2007**, *6*, 858.

217. Balandin, A. A. *Nat. Mater.* **2011**, *10*, 569.

218. Pinto, A. M.; Cabral, J.; D. A. Pacheco Tanaka, Mendes, A. M.; Magalhães, F. D. *Polym. Int.* **2012**, *62*, 33.

219. Mahmoudian, S.; Wahit, M. U.; Imran, M.; Ismail, A. F.; Balakrishnan, H. *J. Nanosci. Nanotechnol.* **2012**, *12*, 5233.

220. Kim, H. M.; Lee, J. K.; Lee, H. S. *Thin Solid Films* **2011**, *519*, 7766.

221. Shim, S. H.; Kim, K. T.; Lee, J. U.; Jo, W. H. *Am. Chem. Soc. Appl. Mater. Interfaces* **2012**, *4*, 4184.

222. Al-Jabareen, A.; Al-Bustami, H.; Harel, H.; Marom, G. *J. Appl. Polym. Sci.* **2012**, *128*, 1534.

223. Prusty, G.; Swain, S. K. *Polym. Compos.* **2011**, *32*, 1336.

224. Chang, C. H.; Huang, T. C.; Peng, C. W.; Yeh, T. C.; Lu, H. I.; Hung, W. I.; Weng, C. J.; Yang, T. I.; Yeh, J. M. *Carbon* **2012**, *50*, 5044.

225. Paredes, J. I.; Villar-Rodil, S.; Martinez-Alonso, A.; Tascon, J. M. D. *Langmuir* **2008**, *24*, 10560.

226. Song, P. A.; Yu, Y. M.; Zhang, T.; Fu, S. Y.; Fang, Z. P.; Wu, Q. *Ind. Eng. Chem. Res.* **2012**, *51*, 7255.

227. Loh, K. P.; Bao, Q. L.; Ang, P. K.; Yang, J. X. *J. Mater. Chem.* **2010**, *20*, 2277.

228. Geim, A. K. *Science* **2009**, *324*, 1530.

229. Terrones, M.; Martin, O.; Gonzalez, M.; Pozuelo, J.; Serrano, B.; Cabanelas, J. C.; Vega-Diaz, S. M.; Baselga, J. *Adv. Mater.* **2011**, *23*, 5302.

230. Kuila, T.; Bose, S.; Mishra, A. K.; Khanra, P.; Kim, N. H.; Lee, J. H. *Polym. Test.* **2012**, *31*, 31.

231. Kelly, B. T. *Carbon* **1972**, *10*, 429.

232. Jeong, H. K.; Lee, Y. P.; Lahaye, R. J. W. E.; Park, M. H.; An, K. H.; Kim, I. J.; Yang, C. W.; Park, C. Y.; Ruoff, R. S.; Lee, Y. H. *J. Am. Chem. Soc.* **2008**, *130*, 1362.

233. Szabó, T.; Berkesi, O.; Forgó, P.; Josepovits, K.; Sanakis, Y.; Petridis, D.; Dékány, I. *Chem. Mater.* **2006**, *18*, 2740.

234. Staudenmaier, L. *Ber. Dtsch. Chem. Ges.* **1898**, *31*, 1481.

235. Hummers, W. S., Jr.; Offeman, R. E. *J. Am. Chem. Soc.* **1958**, *80*, 1339.

236. Kovtyukhova, N. I.; Ollivier, P. J.; Martin, B. R.; Mallouk, T. E.; Chizhik, S. A.; Buzaneva, E. V.; Gorchinskiy, A. D. *Chem. Mater.* **1999**, *11*, 771.

237. Marcano, D. C.; Kosynkin, D. V.; Berlin, J. M.; Sinitskii, A.; Sun, Z.; Slesarev, A.; Alemany, L. B.; Lu, W.; Tour, J. M. *Am. Chem. Soc. Nano* **2010**, *4*, 4806.

238. Kim, H.; Miura, Y.; Macosko, C. W. *Chem. Mater.* **2010**, *22*, 3441.

239. Luong, N. D.; Hippi, U.; Korhonen, J. T.; Soininen, A. J.; Ruokolainen, J.; Johansson, L. S.; Nam, J. D.; Sinh, L. H.; Seppala, J. *Polymer* **2011**, *52*, 5237.

240. Kim, I. H.; Jeong, Y. G. *J. Polym. Sci. Part B: Polym. Phys.* **2010**, *48*, 850.

241. Raghu, A. V.; Lee, Y. R.; Jeong, H. M.; Shin, C. M. *Macromol. Chem. Phys.* **2008**, *209*, 2487.

242. Jiang, X.; Drzal, L. T. *J. Power Sources* **2012**, *218*, 297.

243. Wang, J. Y.; Yang, S. Y.; Huang, Y. L.; Tien, H. W.; Chin, W. K.; Ma, C. C. M. *J. Mater. Chem.* **2011**, *21*, 13569.

244. Hsiao, M. C.; Liao, S. H.; Yen, M. Y.; Teng, C. C.; Lee, S. H.; Pu, N. W.; Wang, C. A.; Sung, Y.; Ger, M. D.; Ma, C. C. M.; Hsiao, M. H. *J. Mater. Chem.* **2010**, *20*, 8496.

245. Morimune, S.; Nishino, T.; Goto, T. *Am. Chem. Soc. Appl. Mater. Interfaces* **2012**, *4*, 3596.

246. Kim, H.; Macosko, C. W. *Macromolecules* **2008**, *41*, 3317.

247. Lee, D.; Choi, M.-C.; Ha, C.-S. *J. Polym. Sci. Part A: Polym. Chem.* **2012**, *50*, 1611.

248. Tang, Z. H.; Wu, X. H.; Guo, B. C.; Zhang, L. Q.; Jia, D. M. *J. Mater. Chem.* **2012**, *22*, 7492.

249. Xu, Y. X.; Hong, W. J.; Bai, H.; Li, C.; Shi, G. Q. *Carbon* **2009**, *47*, 3538.

250. Lin, Y.; Jin, J.; Song, M. *J. Mater. Chem.* **2011**, *21*, 3455.

251. Han, D. L.; Yan, L. F.; Chen, W. F.; Li, W.; Bangal, P. R. *Carbohydr. Polym.* **2011**, *83*, 966.

252. Cai, D. Y.; Yusoh, K.; Song, M. *Nanotechnology* **2009**, *20*, 085712.

253. Yang, J. T.; Wu, M. J.; Chen, F.; Fei, Z. D.; Zhong, M. Q. *J. Supercrit. Fluids* **2011**, *56*, 201.

254. Kulkarni, D. D.; Choi, I.; Singamaneni, S.; Tsukruk, V. V. *Am. Chem. Soc. Nano* **2010**, *4*, 4667.

255. Liang, J. J.; Huang, Y.; Zhang, L.; Wang, Y.; Ma, Y. F.; Guo, T. Y.; Chen, Y. S. *Adv. Funct. Mater.* **2009**, *19*, 2297.

256. Satti, A.; Larpent, P.; Gun'ko, Y. *Carbon* **2010**, *48*, 3376.

257. Fang, M.; Wang, K. G.; Lu, H. B.; Yang, Y. L.; Nutt, S. *J. Mater. Chem.* **2009**, *19*, 7098.

258. Rafiee, M. A.; Rafiee, J.; Wang, Z.; Song, H. H.; Yu, Z. Z.; Koratkar, N. *Am. Chem. Soc. Nano* **2009**, *3*, 3884.

259. Goncalves, G.; Marques, P. A. A. P.; Barros-Timmons, A.; Bdkin, I.; Singh, M. K.; Emami, N.; Gracio, J. *J. Mater. Chem.* **2010**, *20*, 9927.

260. Wang, X.; Hu, Y.; Song, L.; Yang, H.; Xing, W.; Lu, H. *J. Mater. Chem.* **2011**, *21*, 4222.

261. Liu, H.; Li, Y. Q.; Wang, T. M.; Wang, Q. H. *J. Mater. Sci.* **2012**, *47*, 1867.

262. Zhao, X.; Zhang, Q. H.; Chen, D. J.; Lu, P. *Macromolecules* **2010**, *43*, 2357.

263. Wang, J. C.; Wang, X. B.; Xu, C. H.; Zhang, M.; Shang, X. P. *Polym. Int.* **2011**, *60*, 816.

264. Yang, X. M.; Li, L. A.; Shang, S. M.; Tao, X. M. *Polymer* **2010**, *51*, 3431.

265. Potts, J. R.; Lee, S. H.; Alam, An, T. M. J.; Stoller, M. D.; Piner, R. D.; Ruoff, R. S. *Carbon* **2011**, *49*, 2615.

266. El Achaby, M.; Arrakhiz, F. Z.; Vaudreuil, S.; Essassi, E. M.; Qaiss, A. *Appl. Surf. Sci.* **2012**, *258*, 7668.

267. Steurer, P.; Wissert, R.; Thomann, R.; Mulhaupt, R. *Macromol. Rapid Commun.* **2009**, *30*, 316.

268. Vadukumpully, S.; Paul, J.; Mahanta, N.; Valiyaveettil, S. *Carbon* **2011**, *49*, 198.

269. Kalaitzidou, K.; Fukushima, H.; Drzal, L. T. *Carbon* **2007**, *45*, 1446.

270. Kai, W.; Hirota, Y.; Hua, L.; Inoue, Y. *J. Appl. Polym. Sci.* **2008**, *107*, 1395.

271. Xu, C. X.; Cao, Y. C.; Kumar, R.; Wu, X.; Wang, X.; Scott, K. *J. Mater. Chem.* **2011**, *21*, 11359.

272. Patole, A. S.; Patole, S. P.; Kang, H.; Yoo, J. B.; Kim, T. H.; Ahn, J. H. *J. Colloid Interface Sci.* **2010**, *350*, 530.

273. Wei, T.; Luo, G. L.; Fan, Z. J.; Zheng, C.; Yan, J.; Yao, C. Z.; Li, W. F.; Zhang, C. *Carbon* **2009**, *47*, 2296.

274. Wu, H.; Drzal, L. T. *Carbon* **2012**, *50*, 1135.

275. Wu, J.; Tang, Q.; Sun, H.; Lin, J.; Ao, H.; Huang, M.; Huang, Y. *Langmuir* **2008**, *24*, 4800.

276. Wang, H. L.; Hao, Q. L.; Yang, X. J.; Lu, L. D.; Wang, X. *Am. Chem. Soc. Appl. Mater. Interfaces* **2010**, *2*, 821.

277. Chen, G. H.; Weng, W. G.; Wu, D. J.; Wu, C. L. *Eur. Polym. J.* **2003**, *39*, 2329.

278. Huang, H. D.; Ren, P. G.; Chen, J.; Zhang, W. Q.; Ji, X.; Li, Z. M. *J. Membr. Sci.* **2012**, *409*, 156.

279. Compton, O. C.; Kim, S.; Pierre, C.; Torkelson, J. M.; Nguyen, S. T. *Adv. Mater.* **2010**, *22*, 4759.

280. Tseng, I. H.; Liao, Y. F.; Chiang, J. C.; Tsai, M. H. *Mater. Chem. Phys.* **2012**, *136*, 247.

281. Yang, Y.-H.; Bolling, L.; Priolo, M. A.; Grunlan, J. C. *Adv. Mater.* **2013**, *25*, 503.

282. Yu, L.; Lim, Y. S.; Han, J. H.; Kim, K.; Kim, J. Y.; Choi, S. Y.; Shin, K. *Synth. Met.* **2012**, *162*, 710.

283. Ramanathan, T.; Abdala, A. A.; Stankovich, S.; Dikin, D. A.; Herrera-Alonso, M.; Piner, R. D.; Adamson, D. H.; Schniepp, H. C.; Chen, X.; Ruoff, R. S.; Nguyen, S. T.; Aksay, I. A.; Prud'homme, R. K.; Brinson, L. C. *Nat. Nanotechnol.* **2008**, *3*, 327.

284. Bose, S.; Kuila, T.; Uddin, M. E.; Kim, N. H.; Lau, A. K. T.; Lee, J. H. *Polymer* **2010**, *51*, 5921.

285. Guo, Y. Q.; Bao, C. L.; Song, L.; Yuan, B. H.; Hu, Y. *Ind. Eng. Chem. Res.* **2011**, *50*, 7772.

286. Yu, A. P.; Ramesh, P.; Itkis, M. E.; E. Bekyarova; Haddon, R. C. *J. Phys. Chem. C* **2007**, *111*, 7565.